Supplemental Figures

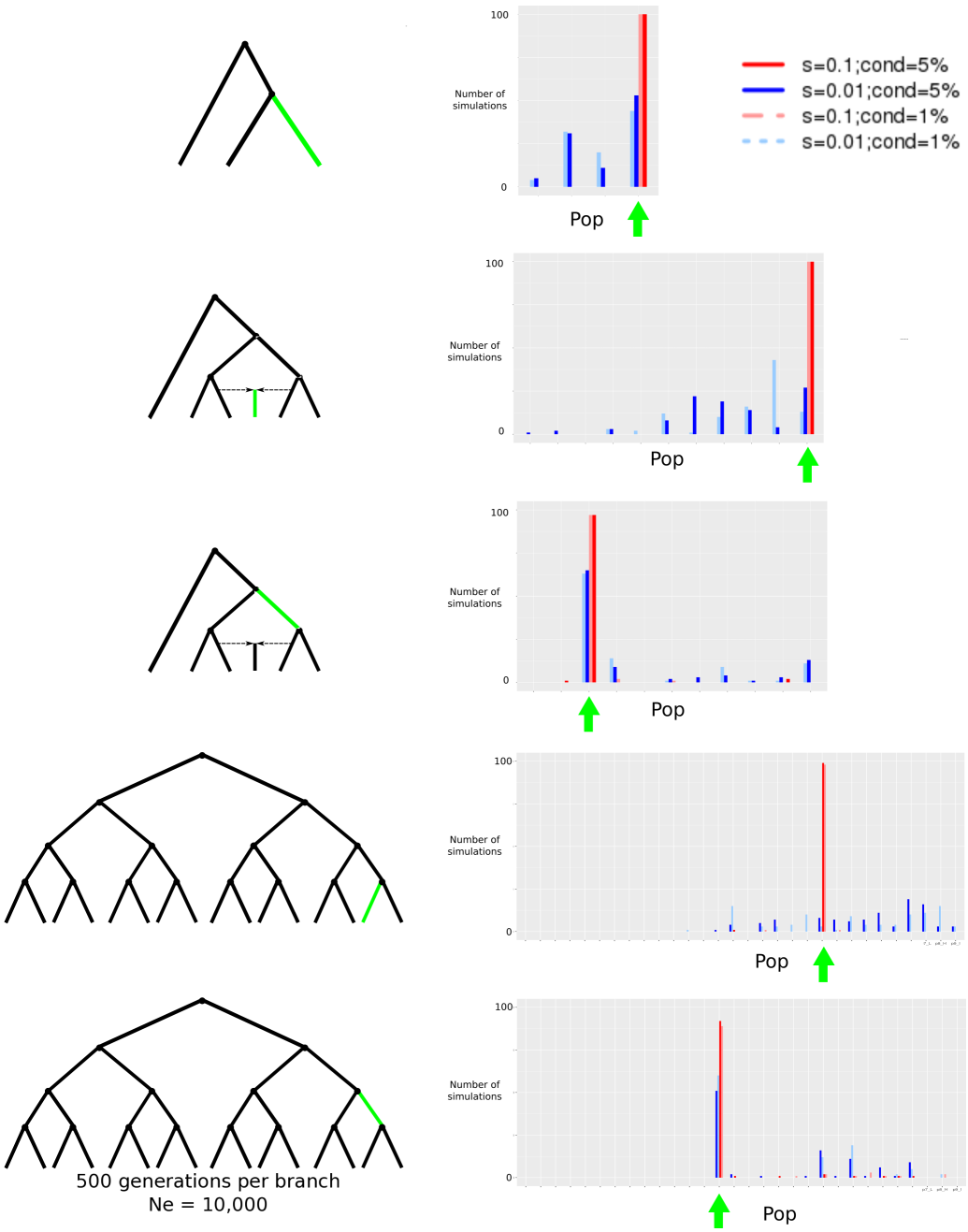

Figure S1: Evaluation of *GRoSS* performance using simulations in *SLiM 2*, with 50 diploid invididuals per population panel. We simulated different selective sweeps under strong (s=0.1) and intermediate (s=0.01) selection coefficients for a 3-population tree, a 6-population graph with a 50%/50% admixture event and a 16-population tree. We obtained the maximum branch score within 100kb of the selected site, and computed the number of simulations (out of 100) in which the branch of this score corresponded to the true branch in which the selected mutation arose (highlighted in green). "$cond = 5\%$": Simulations conditional on the beneficial mutation reaching 5% frequency or more. "$cond = 1\%$": Simulations conditional on the beneficial mutation reaching 1% frequency or more. "Pop": population branch. The green arrow denotes the values of the statistic corresponding to the branch in which the selected mutation arose.

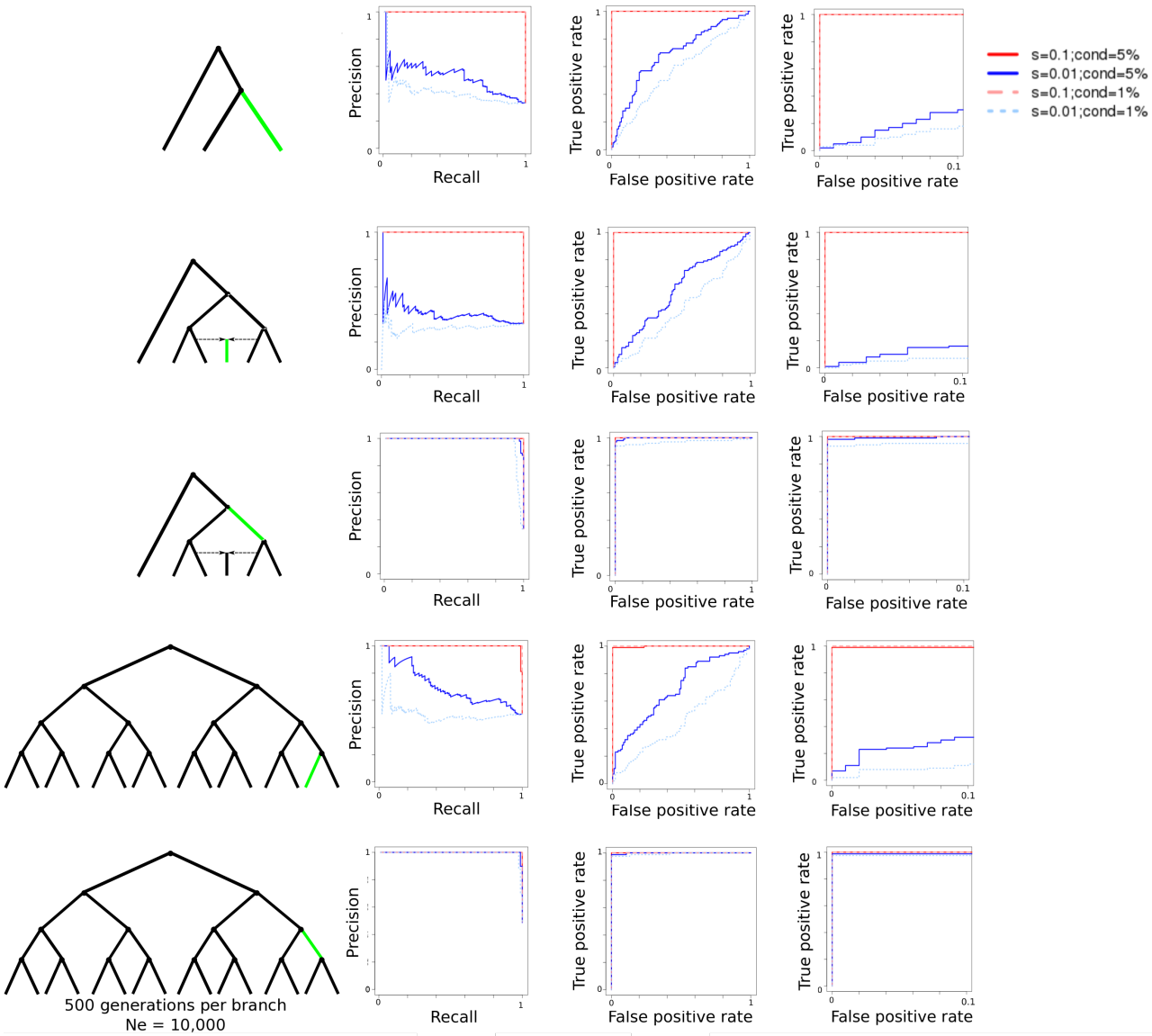

Figure S2: Evaluation of *GRoSS* performance using simulations in *SLiM 2*, with 50 diploid individuals per population panel. We produced precision-recall (left panel) and ROC curves (center and right panels) comparing simulations under selection to simulations under neutrality for a 3-population tree, a 6-population graph with a 50%/50% admixture event and a 16-population tree. The right-most ROC curves are a zoomed-in version of the center ROC curves, in which the false positive rate is limited to be equal to or less than 0.1.

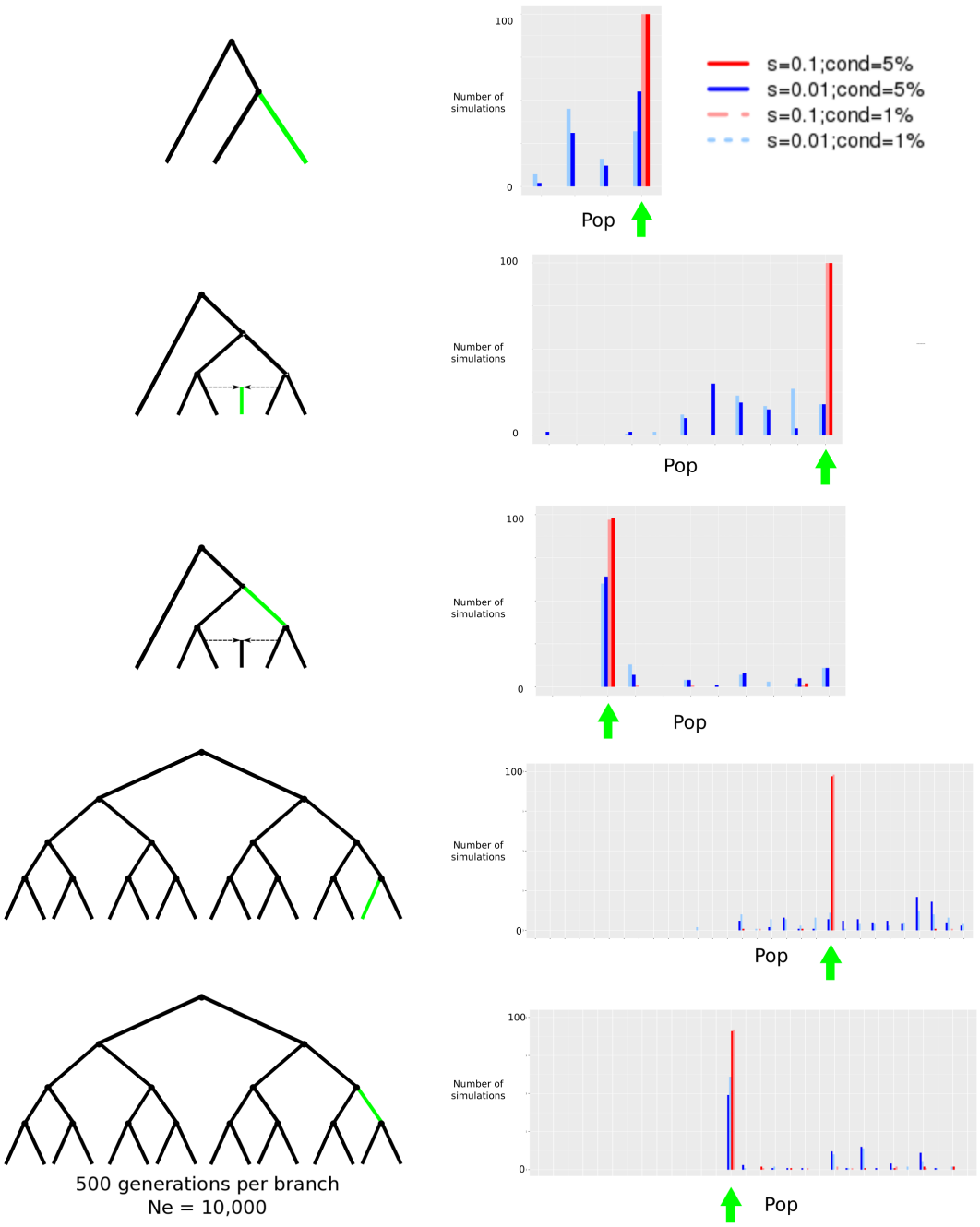

Figure S3: Evaluation of *GRoSS* performance using simulations in *SLiM 2*, with 25 diploid individuals per population panel. Unless otherwise stated, we simulated different selective sweeps under strong (s=0.1) and intermediate (s=0.01) selection coefficients for a 3-population tree, a 6-population graph with a 50%/50% admixture event and a 16-population tree. We obtained the maximum branch score within 100kb of the selected site, and computed the number of simulations (out of 100) in which the branch of this score corresponded to the true branch in which the selected mutation arose (highlighted in green). "*cond* = 5%": Simulations conditional on the beneficial mutation reaching 5% frequency or more. "*cond* = 1%": Simulations conditional on the beneficial mutation reaching 1% frequency or more. "Pop": population branch. The green arrow denotes the values of the statistic corresponding to the branch in which the selected mutation arose.

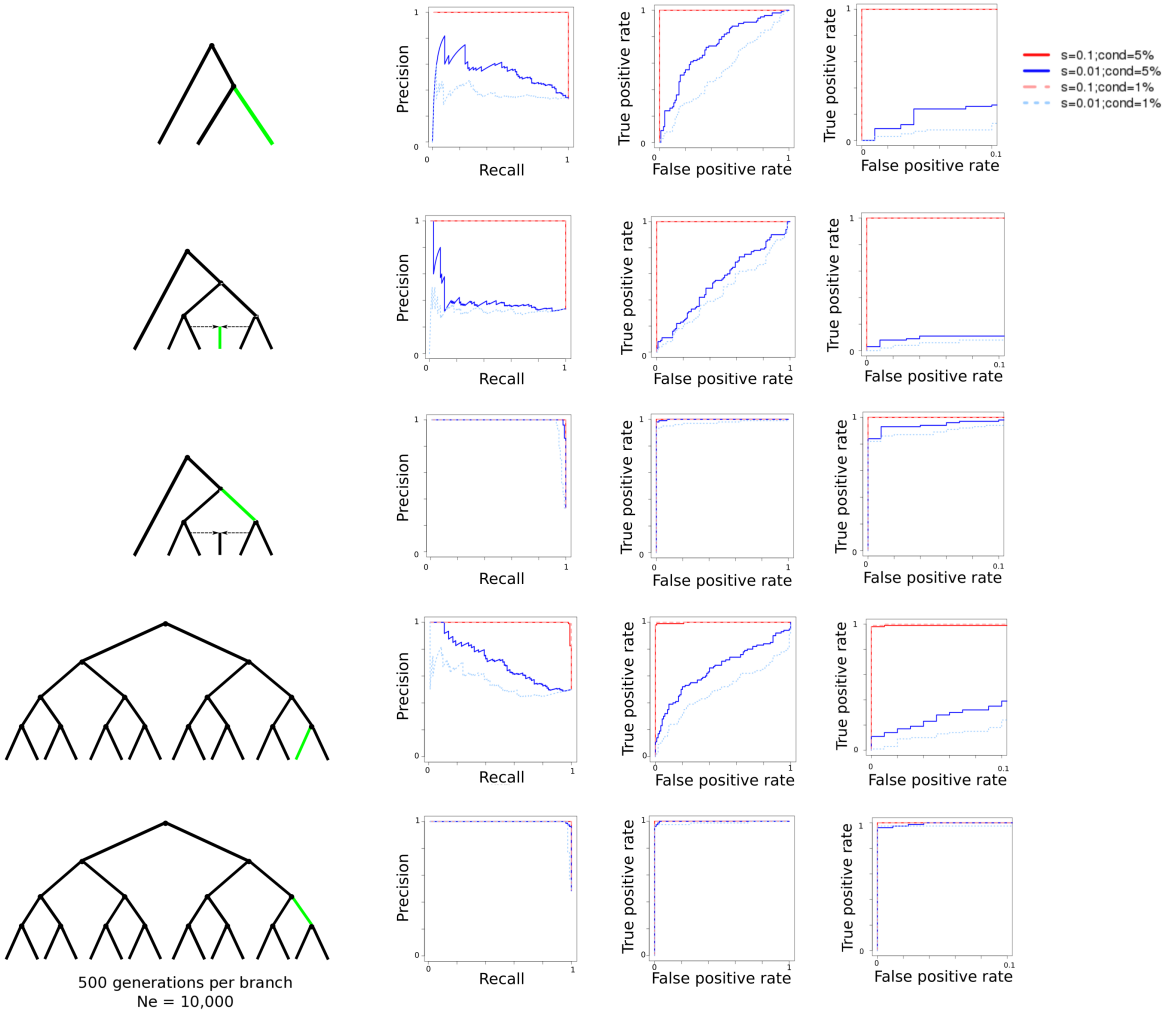

Figure S4: Evaluation of *GRoSS* performance using simulations in *SLiM 2*, with 25 diploid individuals per population panel. We produced precision-recall (left panel) and ROC curves (center and right panels) comparing simulations under selection to simulations under neutrality for a 3-population tree, a 6-population graph with a 50%/50% admixture event and a 16-population tree. The right-most ROC curves are a zoomed-in version of the center ROC curves, in which the false positive rate is limited to be equal to or less than 0.1.

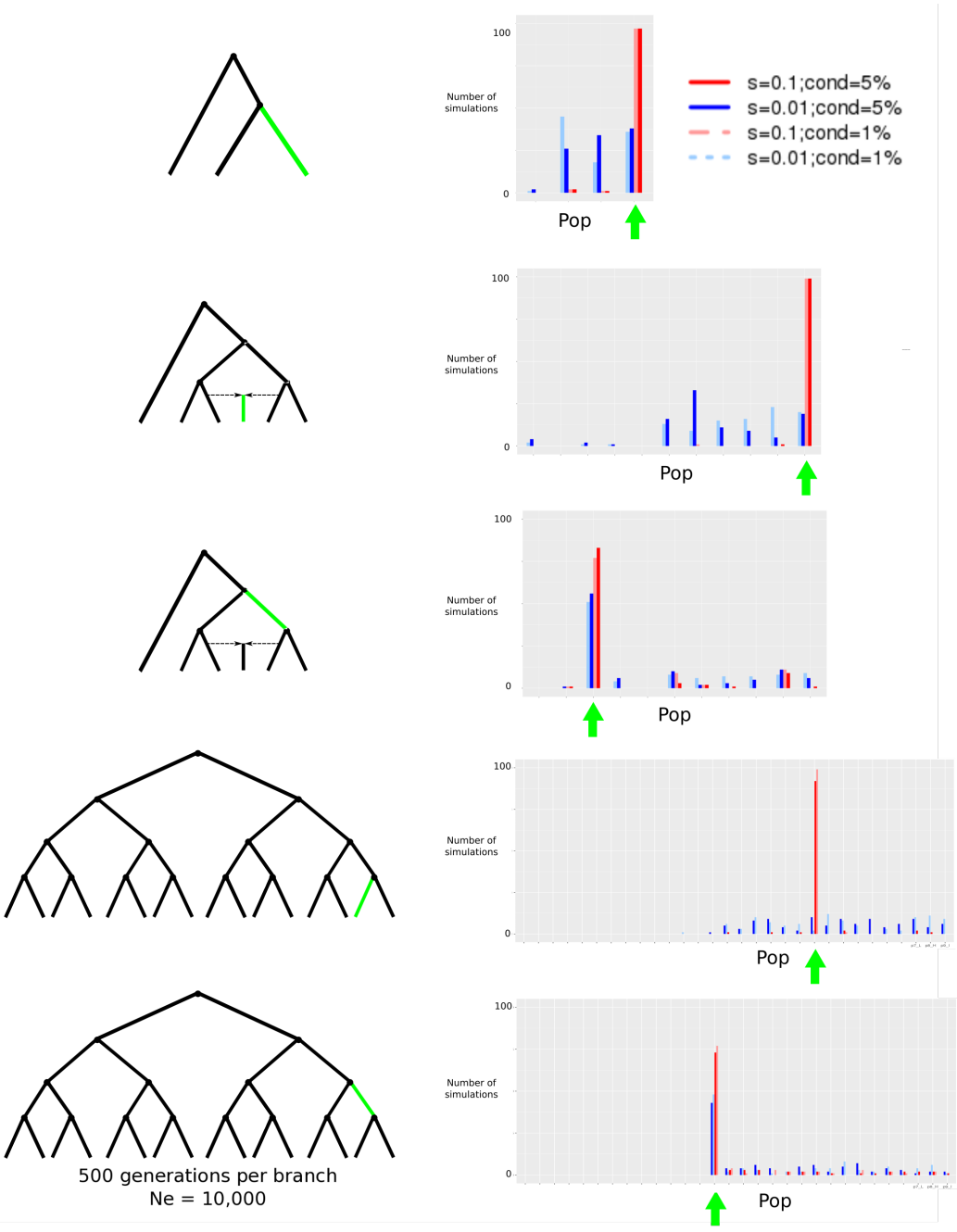

Figure S5: Evaluation of *GRoSS* performance using simulations in *SLiM 2*, with 4 diploid individuals per population panel. We simulated different selective sweeps under strong (s=0.1) and intermediate (s=0.01) selection coefficients for a 3-population tree, a 6-population graph with a 50%/50% admixture event and a 16-population tree. We obtained the maximum branch score within 100kb of the selected site, and computed the number of simulations (out of 100) in which the branch of this score corresponded to the true branch in which the selected mutation arose (highlighted in green). "$cond = 5\%$": Simulations conditional on the beneficial mutation reaching 5% frequency or more. "$cond = 1\%$": Simulations conditional on the beneficial mutation reaching 1% frequency or more. "Pop": population branch. The green arrow denotes the values of the statistic corresponding to the branch in which the selected mutation arose.

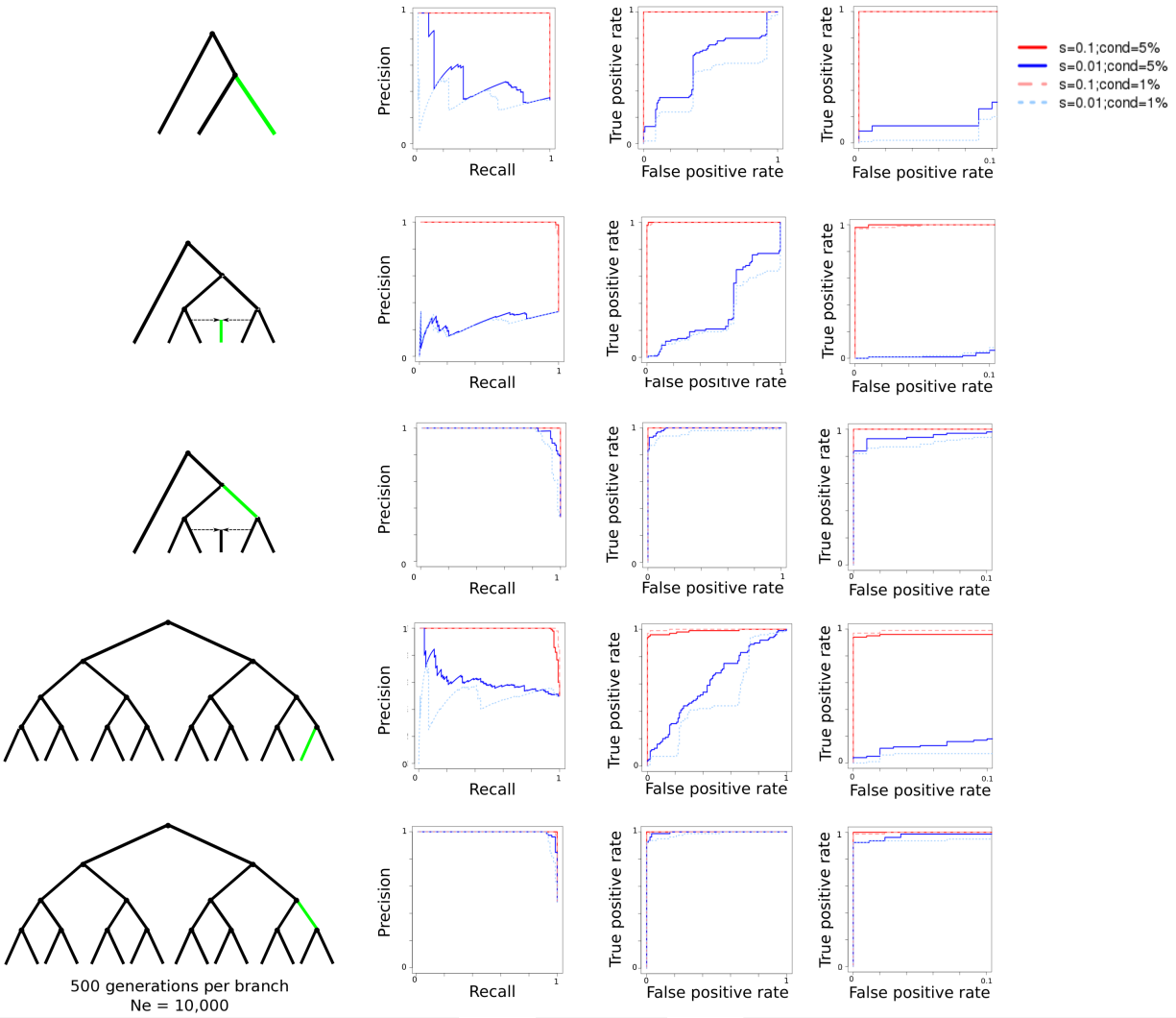

Figure S6: Evaluation of *GRoSS* performance using simulations in *SLiM 2*, with 4 diploid individuals per population panel. We produced precision-recall (left panel) and ROC curves (center and right panels) comparing simulations under selection to simulations under neutrality for a 3-population tree, a 6-population graph with a 50%/50% admixture event and a 16-population tree. The right-most ROC curves are a zoomed-in version of the center ROC curves, in which the false positive rate is limited to be equal to or less than 0.1.

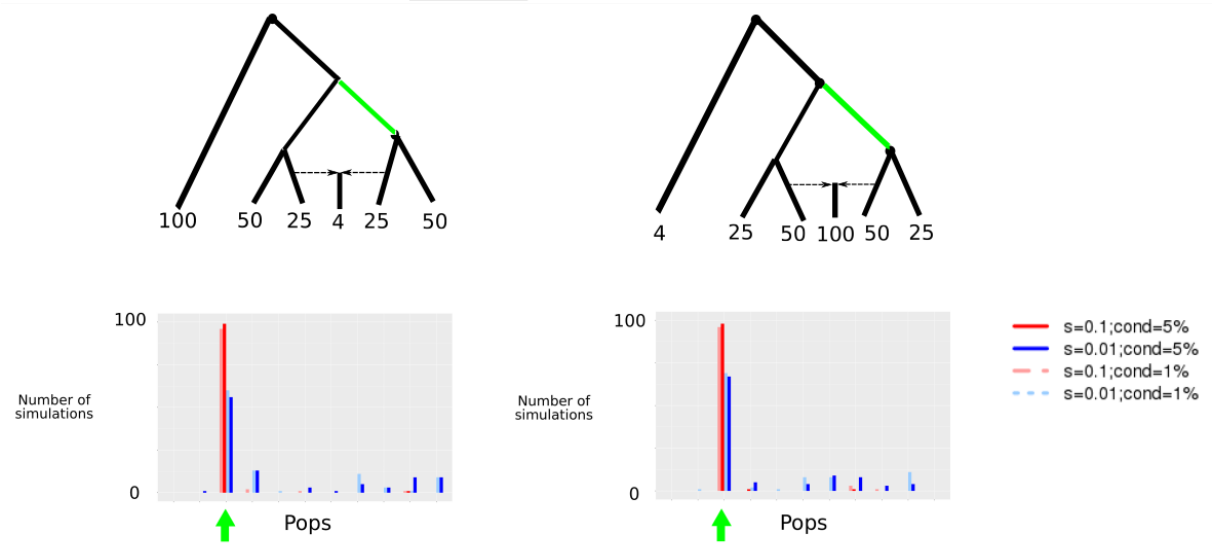

Figure S7: We compared simulations under different selection coefficients, s, and minimum mutation establishment, *cond*, for two scenarios in which we sampled different numbers of individuals from each of the leaf populations. For each of the 100 simulations under each scenario, we obtained the maximum branch score within 100kb of the selected site, and computed the number of simulations (out of 100) in which the branch of this score corresponded to the true branch in which the selected mutation arose (highlighted in green). The green arrow denotes the values of the statistic corresponding to the branch in which the selected mutation arose.

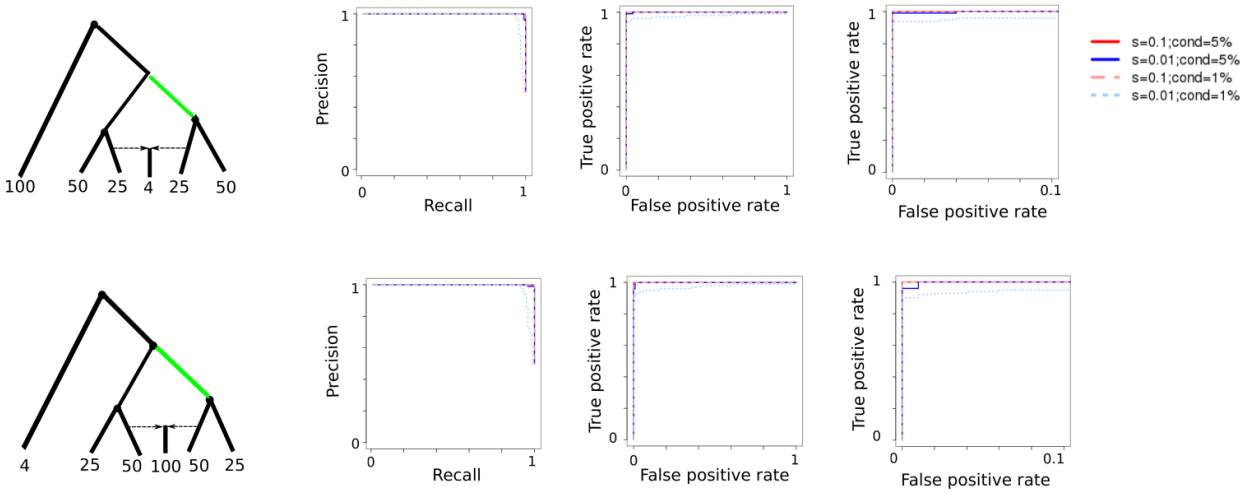

Figure S8: We produced precision-recall (left panel) and ROC curves (center and right panels) comparing simulations under selection to simulations under neutrality for two scenarios in which we sampled different numbers of individuals from each of the leaf populations. The right-most ROC curves are a zoomed-in version of the center ROC curves, in which the false positive rate is limited to be equal to or less than 0.1.

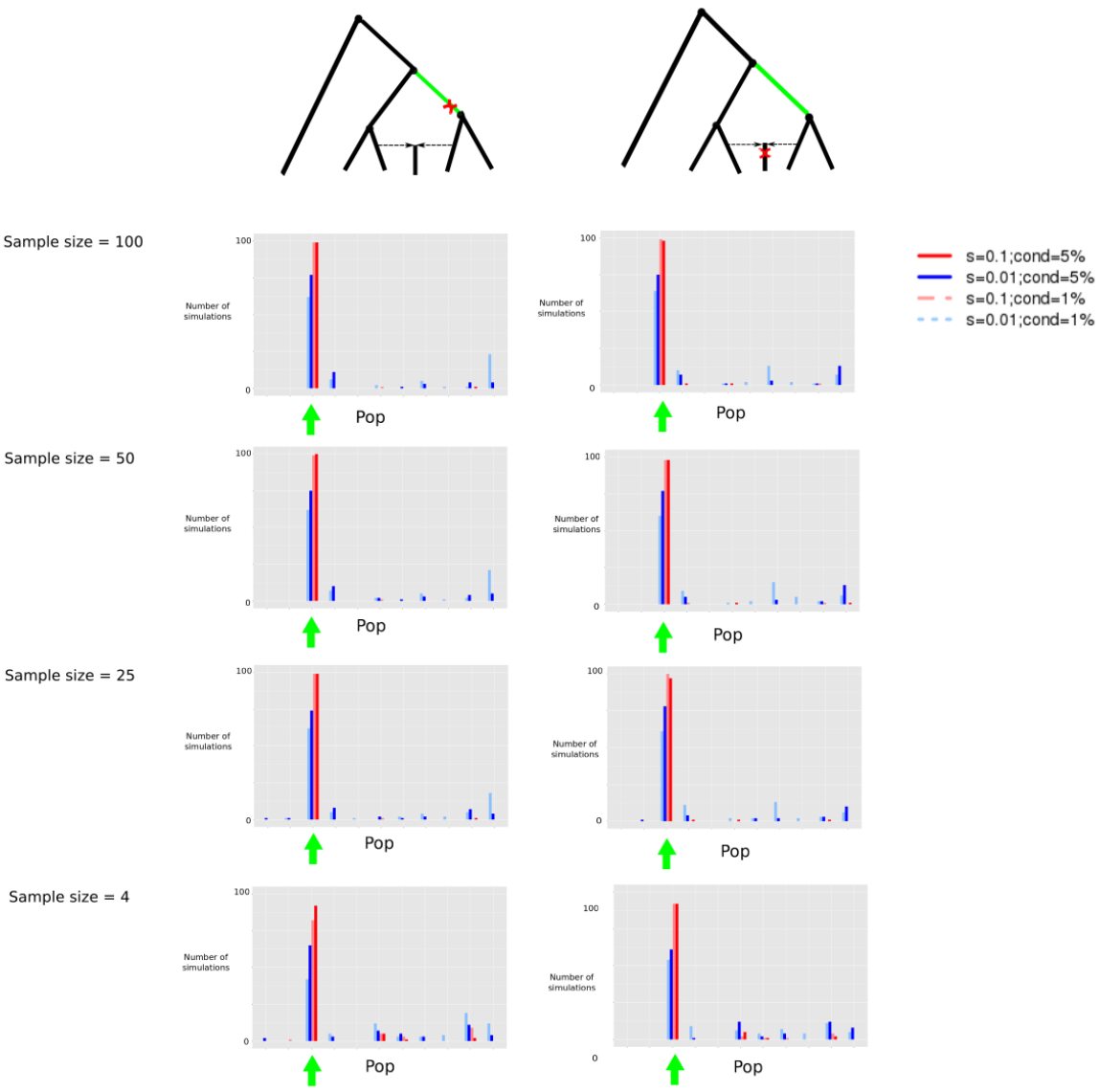

Figure S9: We compared simulations under different selection coefficients, s, and minimum mutation establishment, *cond*, for two scenarios in which we simulated a 5X bottleneck lasting 10 generations (red cross) in different branches of a 6-population graph. For each of the 100 simulations under each scenario, we obtained the maximum branch score within 100kb of the selected site, and computed the number of simulations (out of 100) in which the branch of this score corresponded to the true branch in which the selected mutation arose (highlighted in green). The green arrow denotes the values of the statistic corresponding to the branch in which the selected mutation arose.

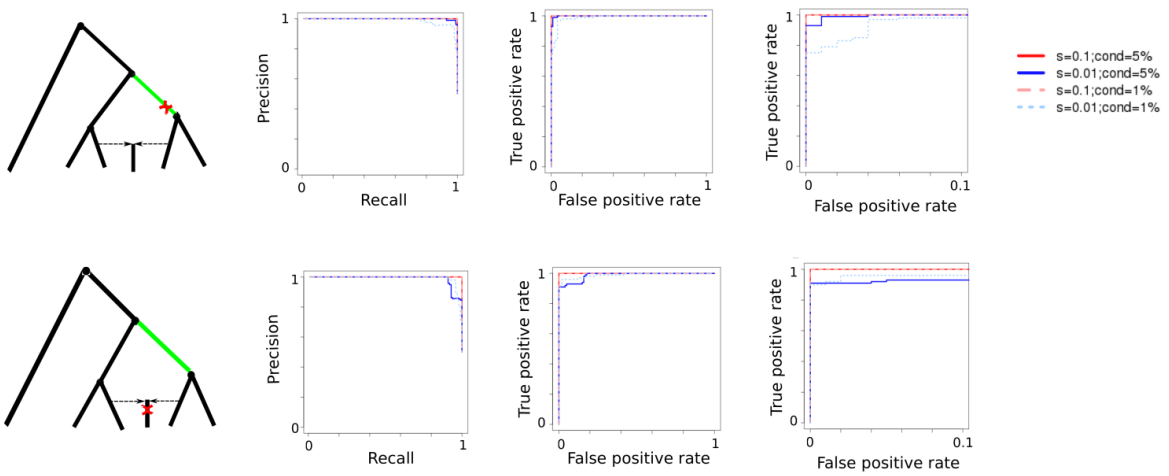

Figure S10: We produced precision-recall (left panel) and ROC curves (center and right panels) comparing simulations under selection to simulations under neutrality for two scenarios in which we simulated a 5X bottleneck lasting 10 generations (red cross) in different branches of a 6-population graph. The sample size for each leaf population was 100 diploid genomes.

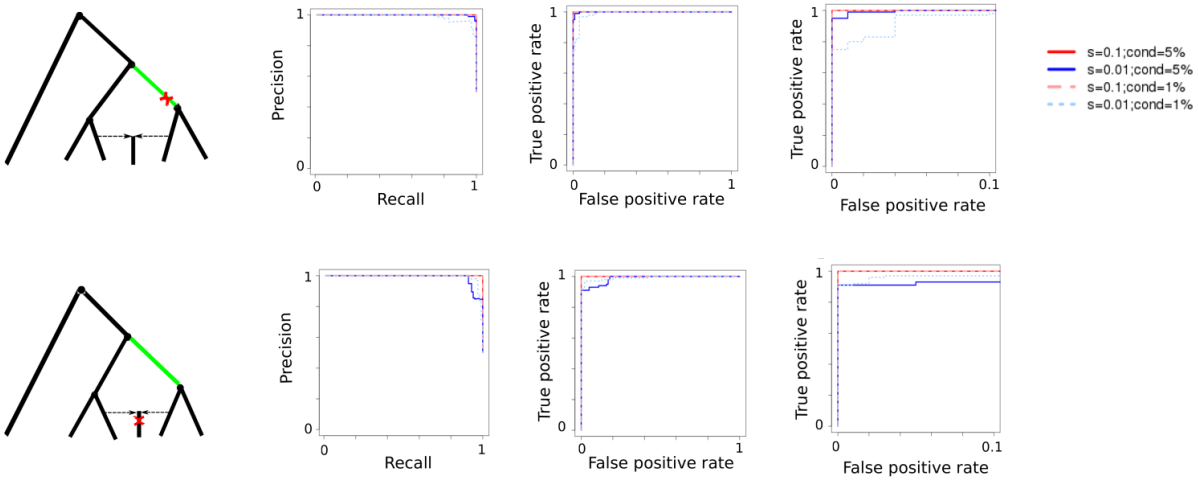

Figure S11: We produced precision-recall (left panel) and ROC curves (center and right panels) comparing simulations under selection to simulations under neutrality for two scenarios in which we simulated a 5X bottleneck lasting 10 generations (red cross) in different branches of a 6-population graph. The sample size for each leaf population was 50 diploid genomes.

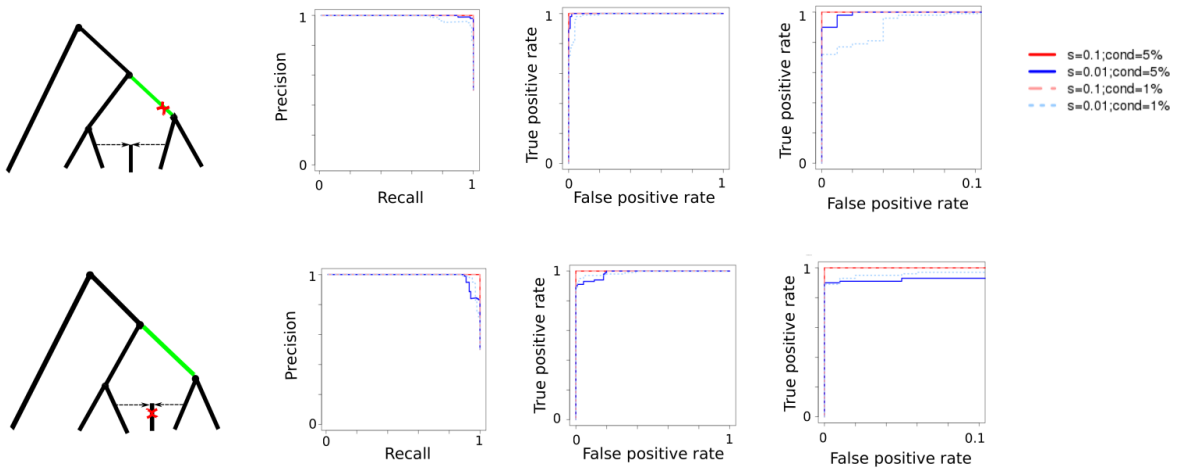

Figure S12: We produced precision-recall (left panel) and ROC curves (center and right panels) comparing simulations under selection to simulations under neutrality for two scenarios in which we simulated a 5X bottleneck lasting 10 generations (red cross) in different branches of a 6-population graph. The sample size for each leaf population was 25 diploid genomes.

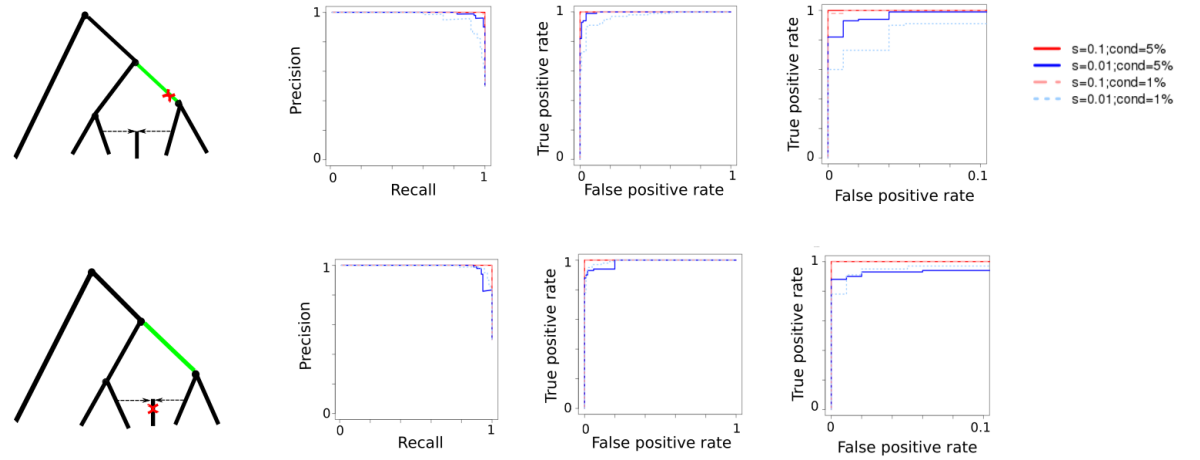

Figure S13: We produced precision-recall (left panel) and ROC curves (center and right panels) comparing simulations under selection to simulations under neutrality for two scenarios in which we simulated a 5X bottleneck lasting 10 generations (red cross) in different branches of a 6-population graph. The sample size for each leaf population was 4 diploid genomes.

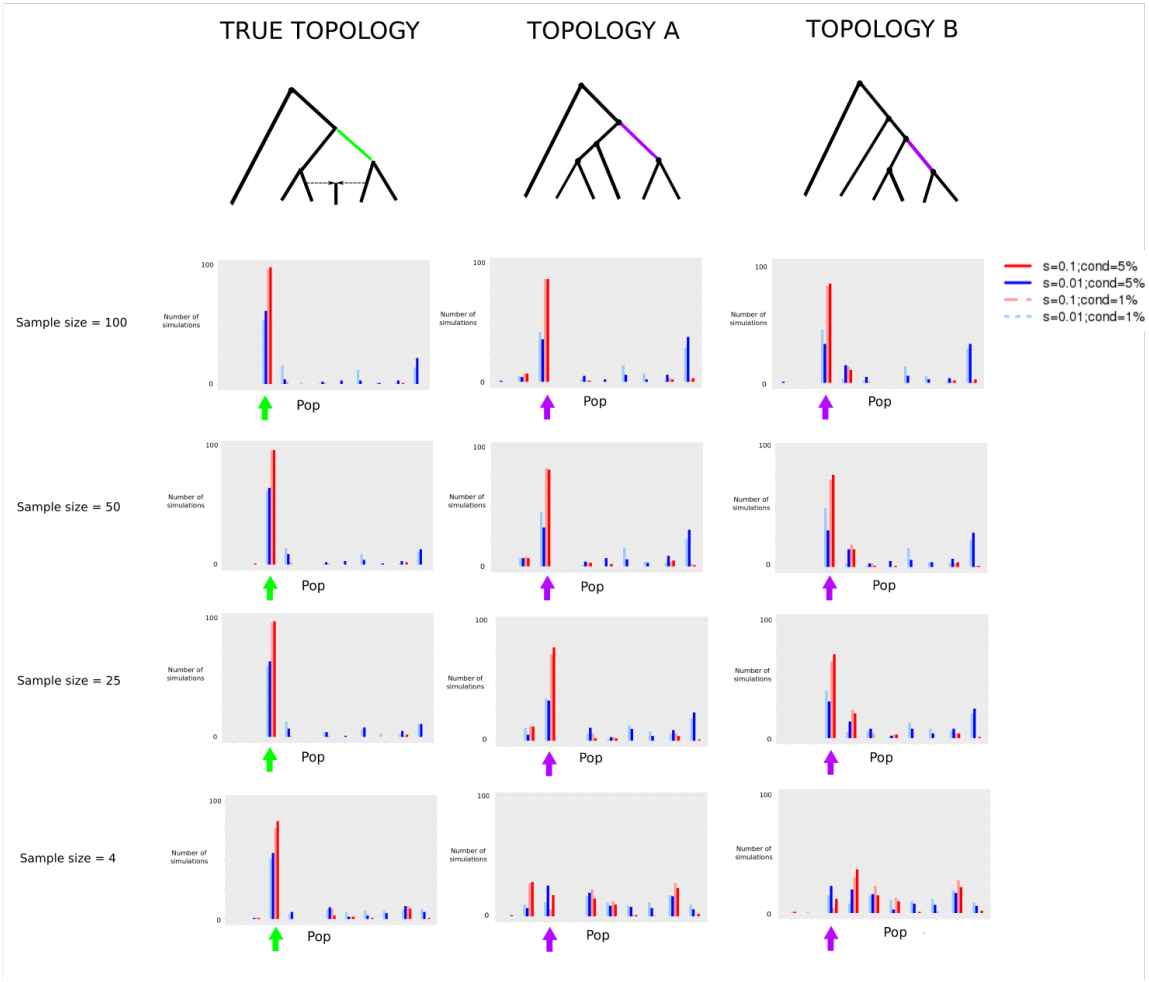

Figure S14: We compared simulations under different selection coefficients, s, and minimum mutation establishment, *cond*, in which we fed *GRoSS* a different 6-population graph topology (A and B) from the one under which we generated the simulations. For each of the 100 simulations under each scenario, we obtained the maximum branch score within 100kb of the selected site, and computed the number of simulations (out of 100) in which the branch of this score corresponded to the true branch in which the selected mutation arose (highlighted in green). The green branch in the true topology is the branch on which the selective event was simulated. The purple branch in each of the wrong topologies is the branch that completely subtends the two populations that are also subtended by the selected branch in the correct graph.

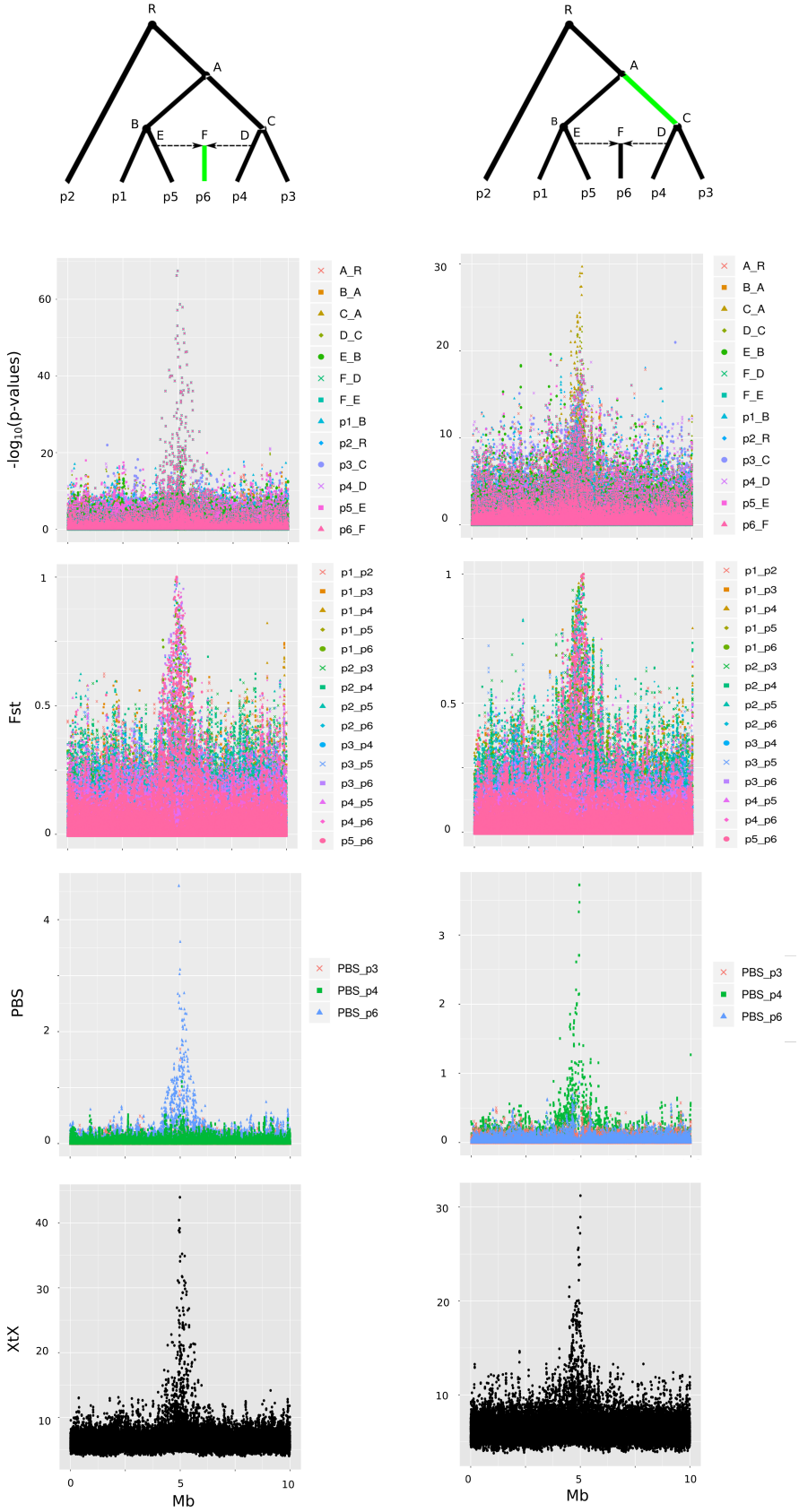

Figure S15: Comparison of population differentiation-based methods used to detect selection. We simulated a strong selective sweep (s=0.1) in two different branches of a 6-population graph with admixture. We then ran *GRoSS* for each branch (first row), pairwise F_{ST} for each population-pair (second row), *PBS* (third row) and the *XtX* statistic from the *BayPass* program (bottom row). Note that all 15 possible pairwise F_{ST} tests are depicted, but only 3 out of the possible 60 *PBS* tests are shown, in the interest of clarity: p3 vs. (p4,p6), p4 vs. (p3,p6) and p6 vs. (p3,p4). These 3 were purposefully chosen such that only one would show a peak at the selected region.

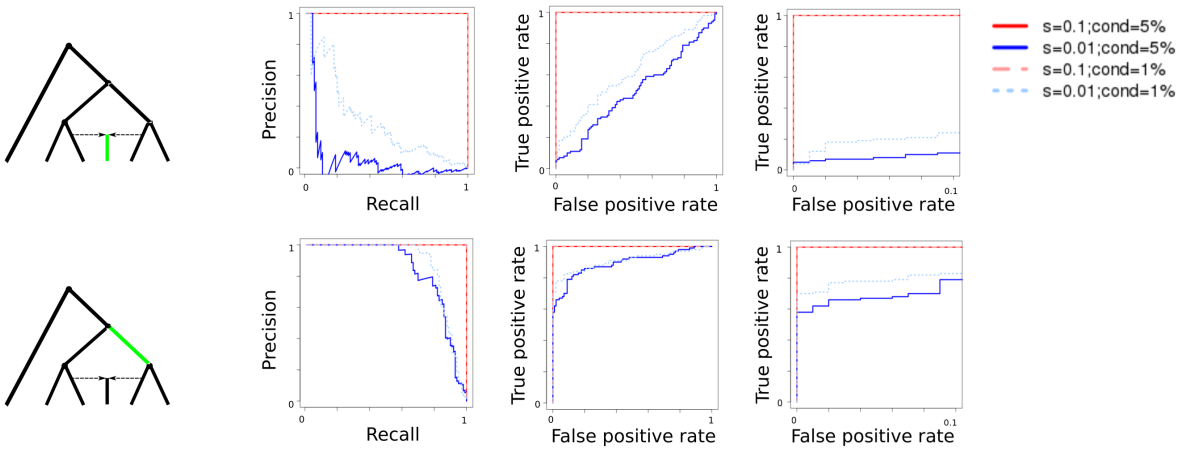

Figure S16: Evaluation of performance of the XtX statistic from *BayPass* using simulations in *SLiM 2*, with 100 diploid individuals per population panel. We produced precision-recall (left panel) and ROC curves (center and right panels) comparing simulations under selection to simulations under neutrality for a 6-population graph with a 50%/50% admixture event. The right-most ROC curves are a zoomed-in version of the center ROC curves, in which the false positive rate is limited to be equal to or less than 0.1.

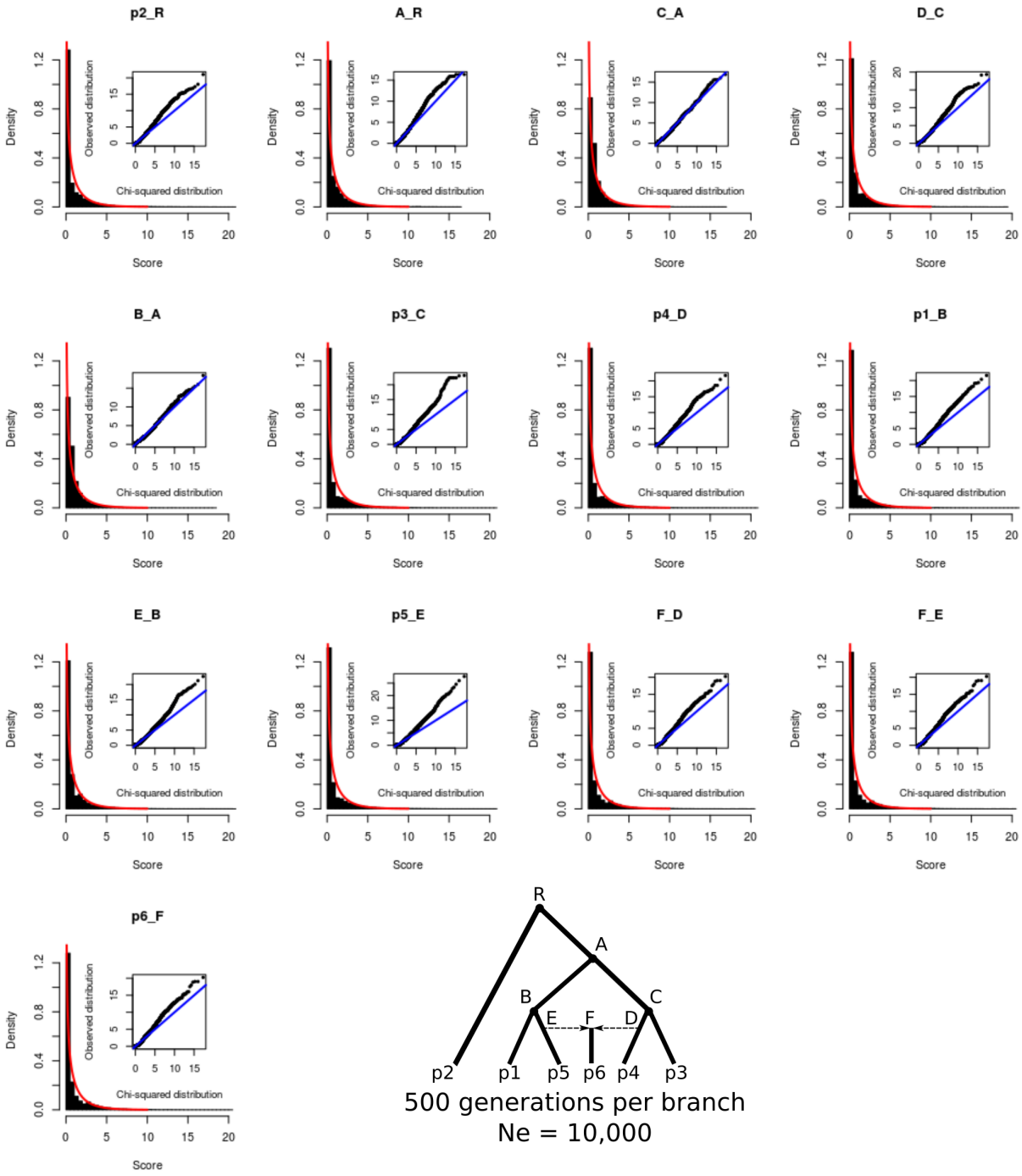

Figure S17: We compared the chi-squared distribution with one degree of freedom (red line) to the actual distribution of S_B scores (histogram) for each branch of a six-population graph with a 50%/50% admixture event under neutrality, sampling 100 diploid individuals per population panel. The inset is a qq-plot of these two distributions. The blue line is the identity line. The titles above each plot denote the parent and child nodes of each branch.

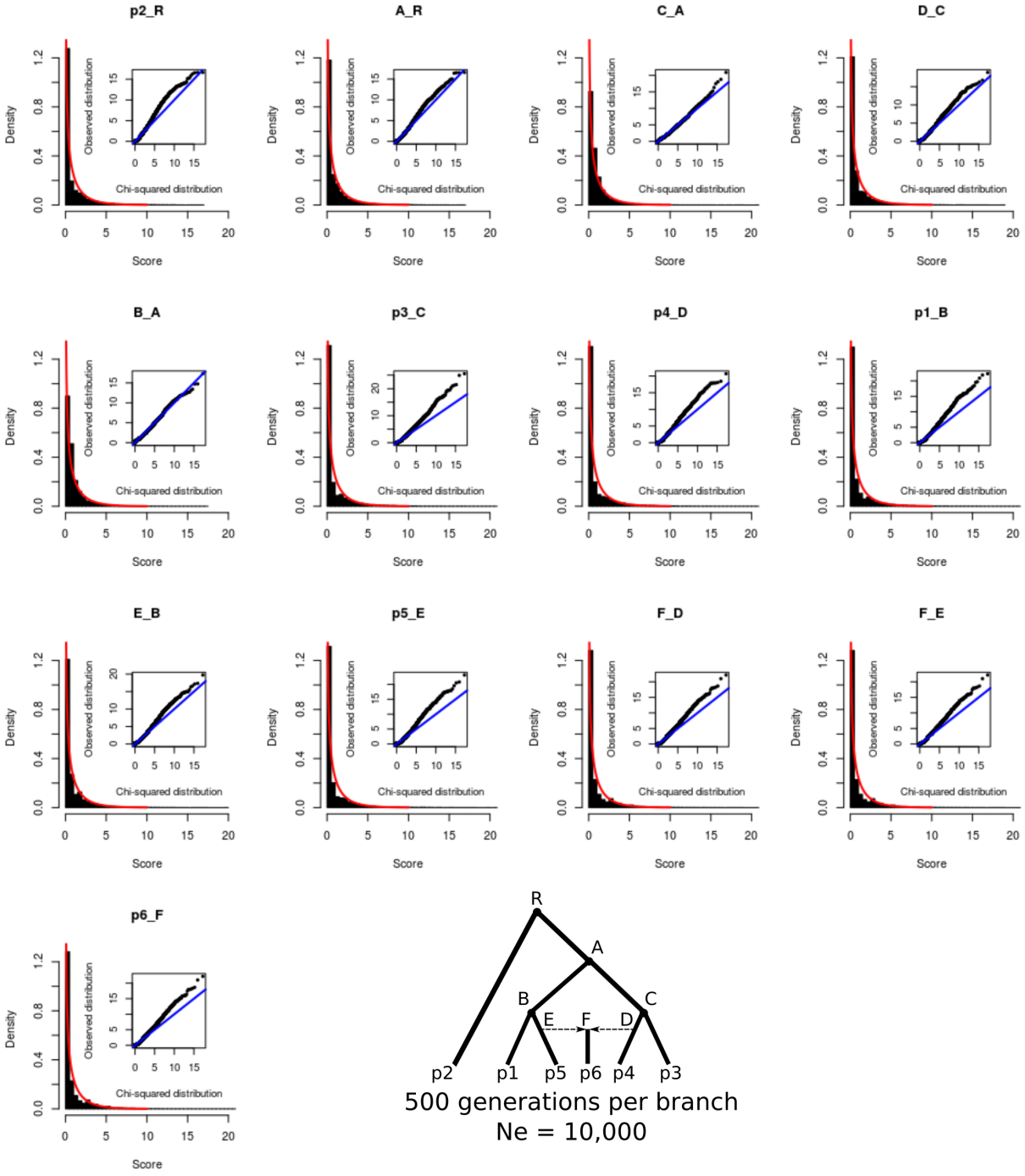

Figure S18: We compared the chi-squared distribution with one degree of freedom (red line) to the actual distribution of S_B scores (histogram) for each branch of a six-population graph with a 50%/50% admixture event under neutrality, sampling 50 diploid individuals per population panel. The inset is a qq-plot of these two distributions. The blue line is the identity line. The titles above each plot denote the parent and child nodes of each branch.

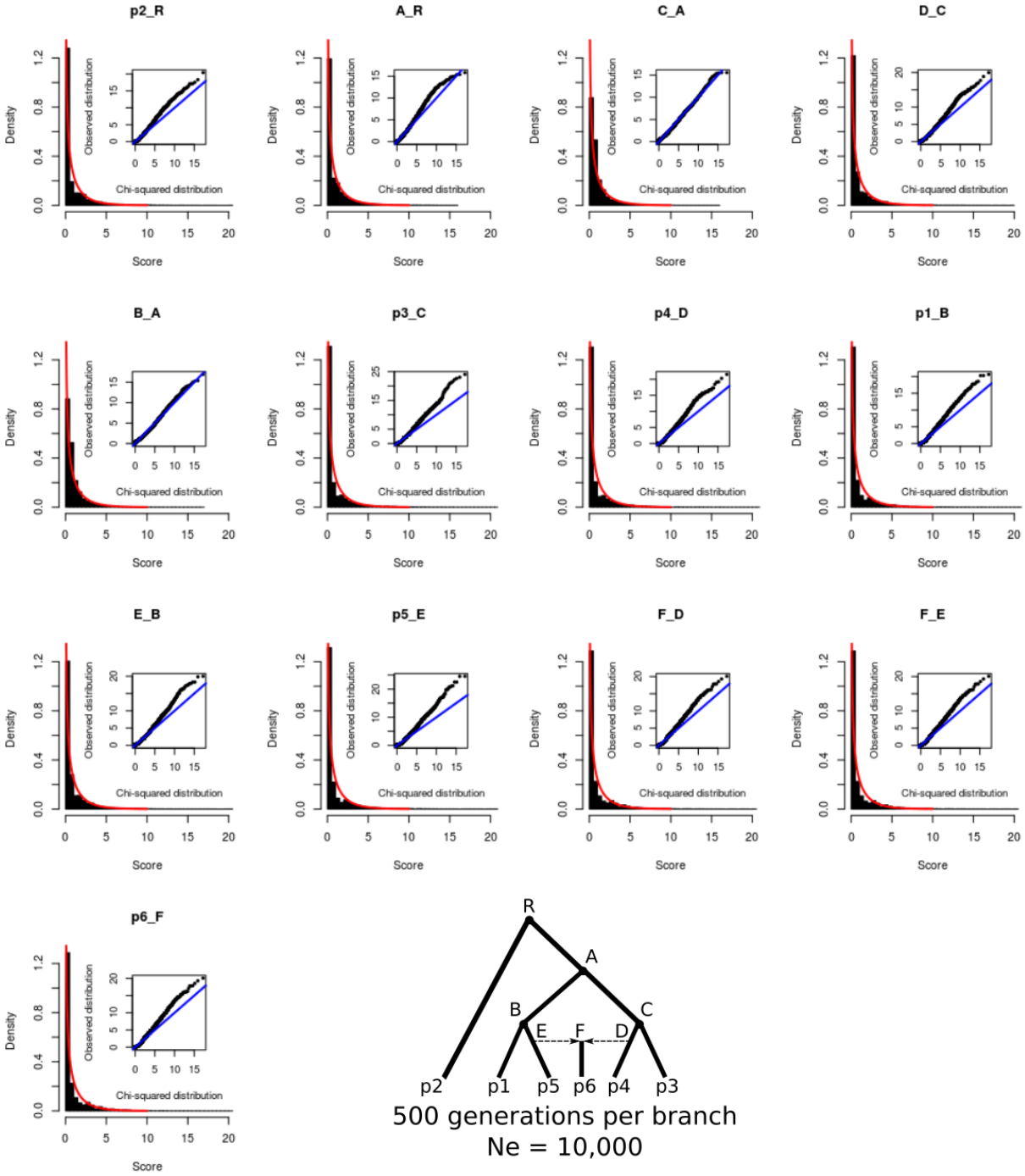

Figure S19: We compared the chi-squared distribution with one degree of freedom (red line) to the actual distribution of S_B scores (histogram) for each branch of a six-population graph with a 50%/50% admixture event under neutrality, sampling 25 diploid individuals per population panel. The inset is a qq-plot of these two distributions. The blue line is the identity line. The titles above each plot denote the parent and child nodes of each branch.

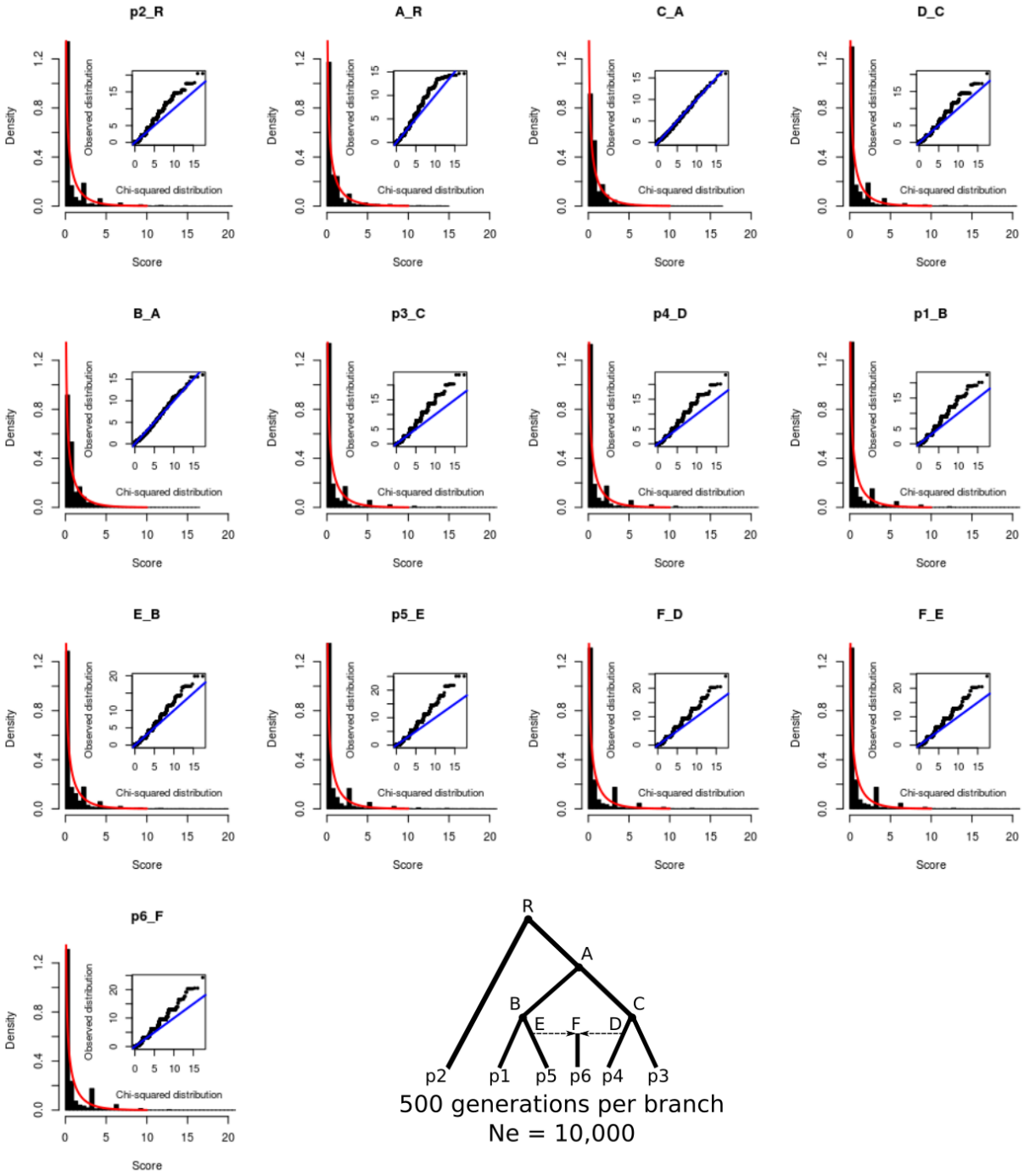

Figure S20: We compared the chi-squared distribution with one degree of freedom (red line) to the actual distribution of S_B scores (histogram) for each branch of a six-population graph with a 50%/50% admixture event under neutrality, sampling 4 diploid individuals per population panel. The inset is a qq-plot of these two distributions. The blue line is the identity line. The titles above each plot denote the parent and child nodes of each branch.

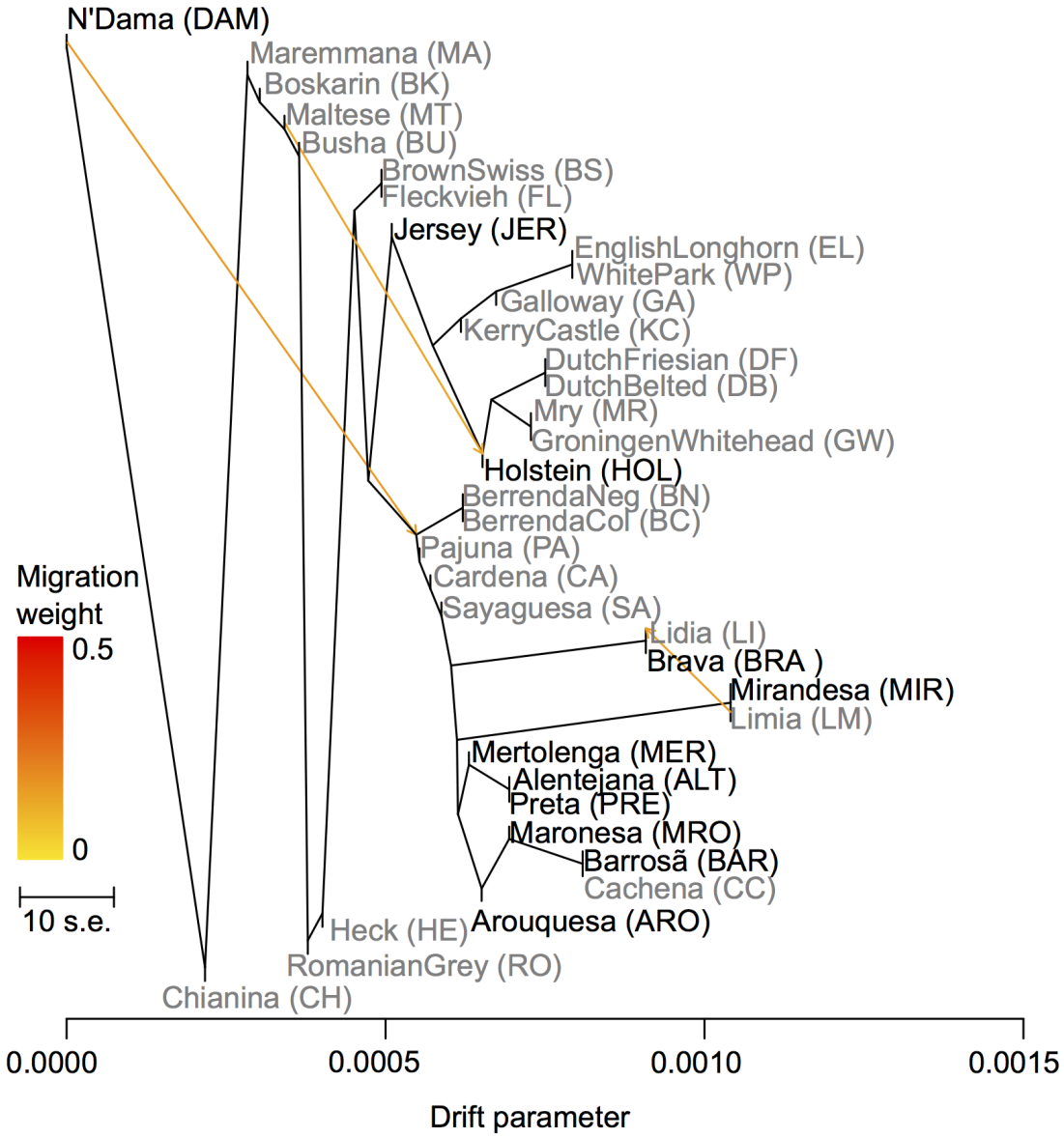

Figure S21: *TreeMix*-fitted maximum likelihood admixture graph with 3 admixture events, depicting the relationships between the taurine cattle breeds analyzed in this study (grey: Illumina BovineHD SNP data; black: whole genome data).

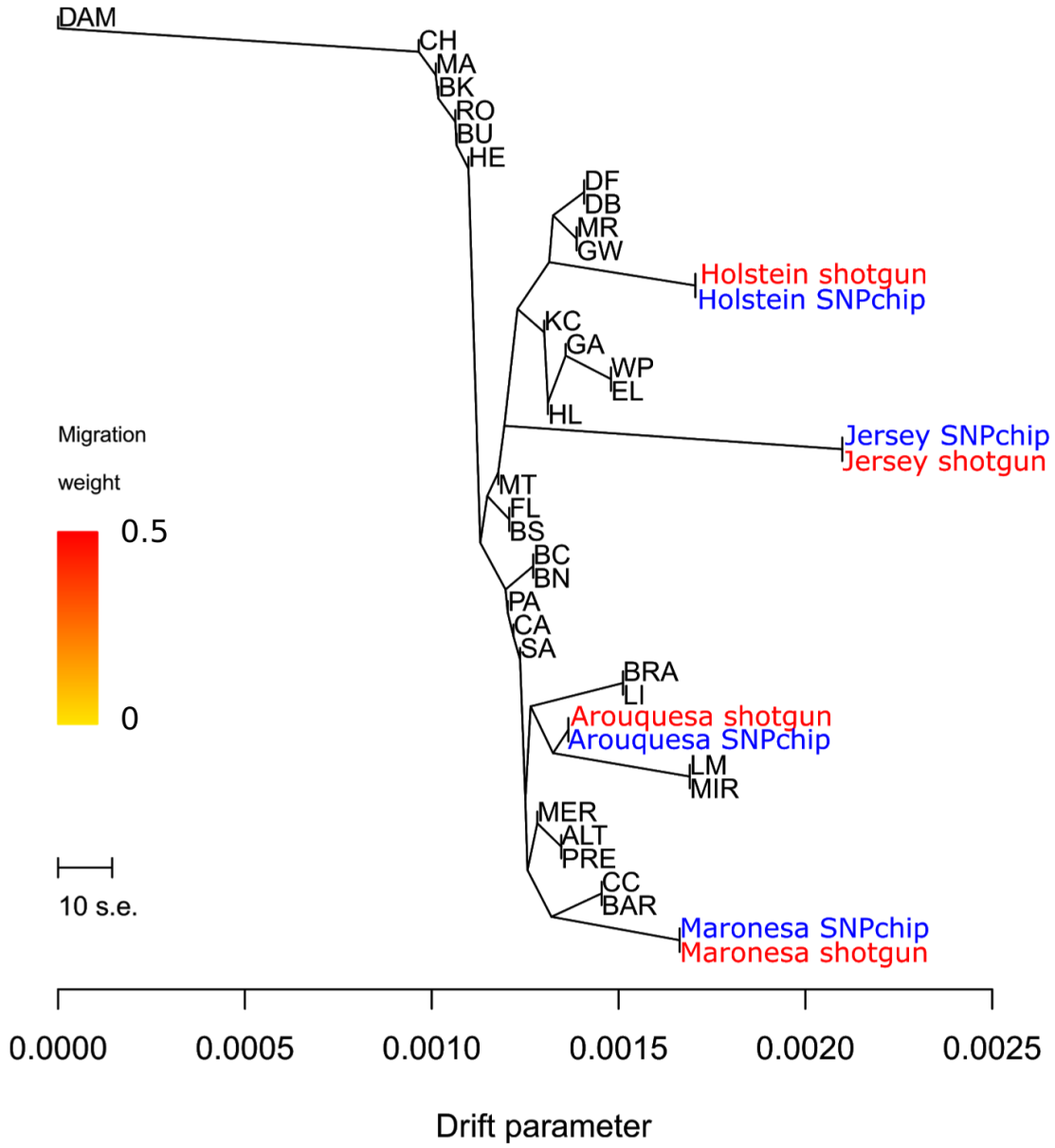

Figure S22: *TreeMix*-fitted maximum likelihood tree, used to test for batch effects between the SNP capture and whole-genome shotgun data, by fitting sequences of the same species that were obtained via both methods.

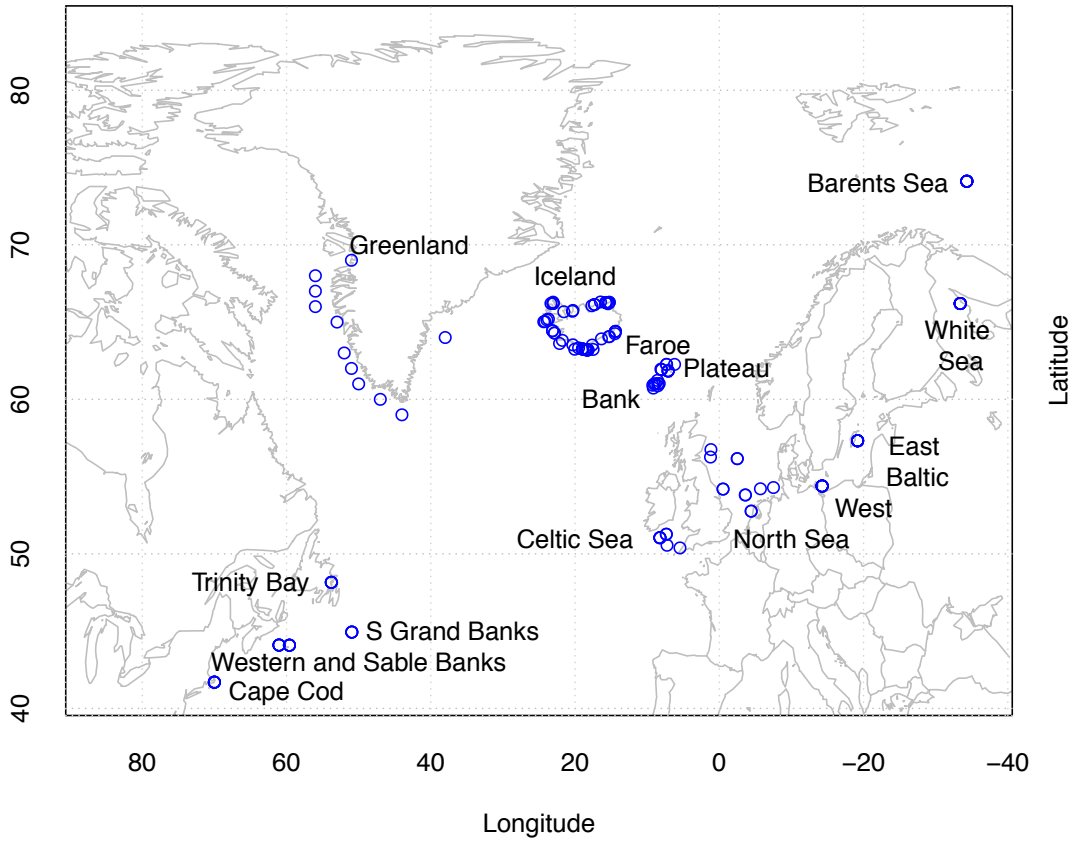

Figure S23: Sample localities of Atlantic cod samples on a map of the North Atlantic.

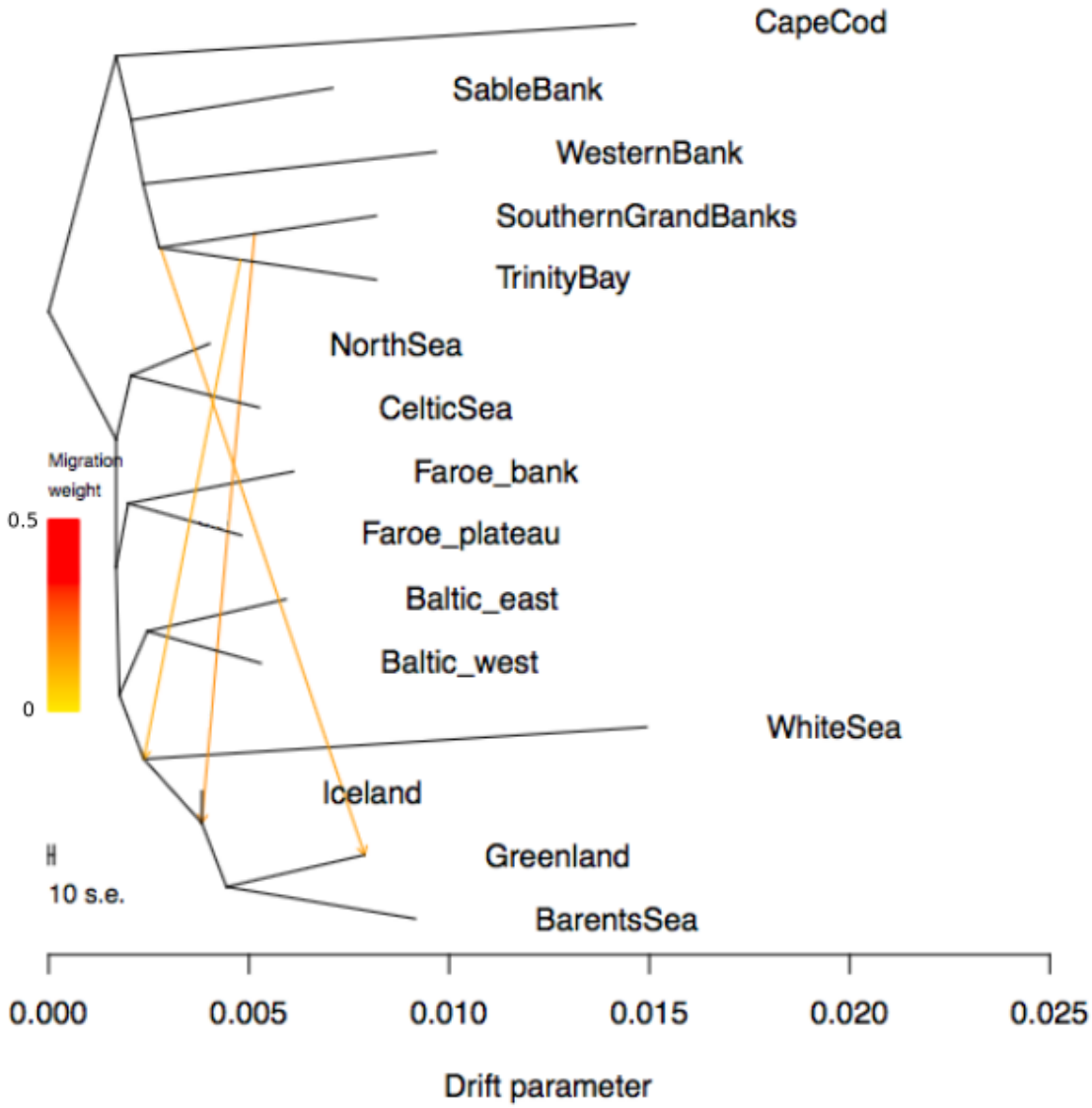

Figure S24: *Treemix*-fitted maximum likelihood admixture graph with 3 admixture events, depicting the relationships between the Atlantic codfish populations.

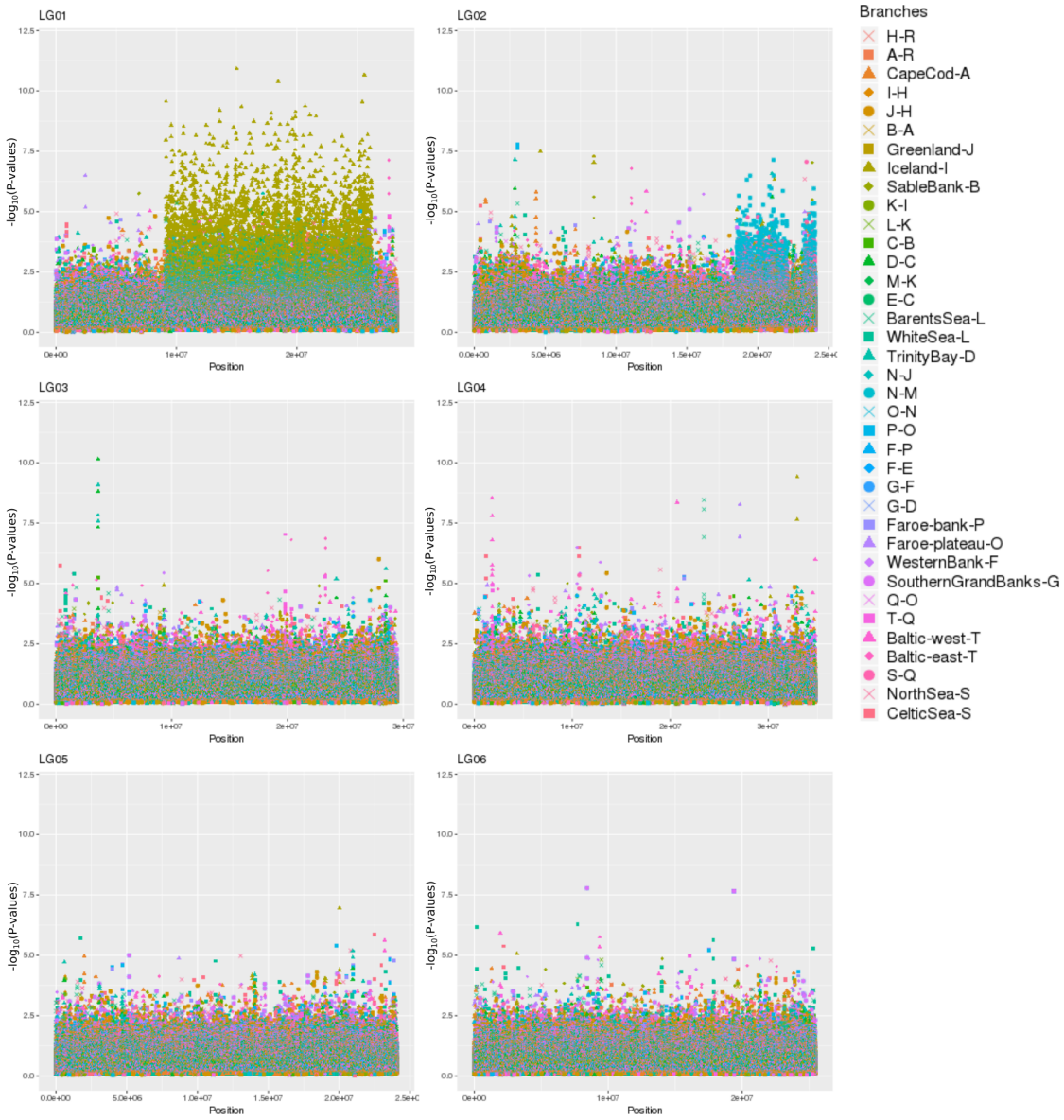

Figure S25: S_B scores for LG01 - LG06 in the Codfish data.

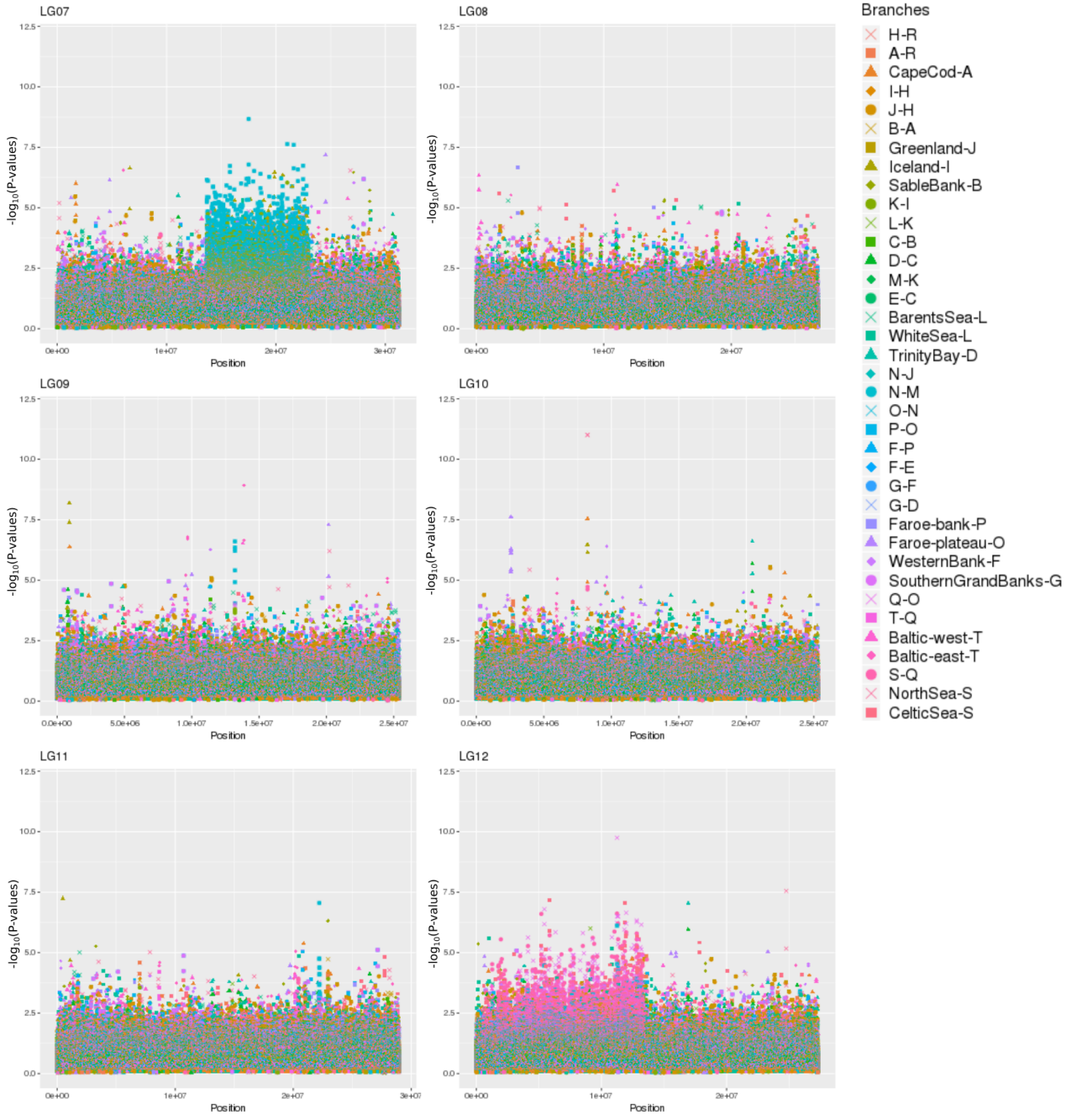

Figure S26: S_B scores for LG07 - LG12 in the Codfish data.

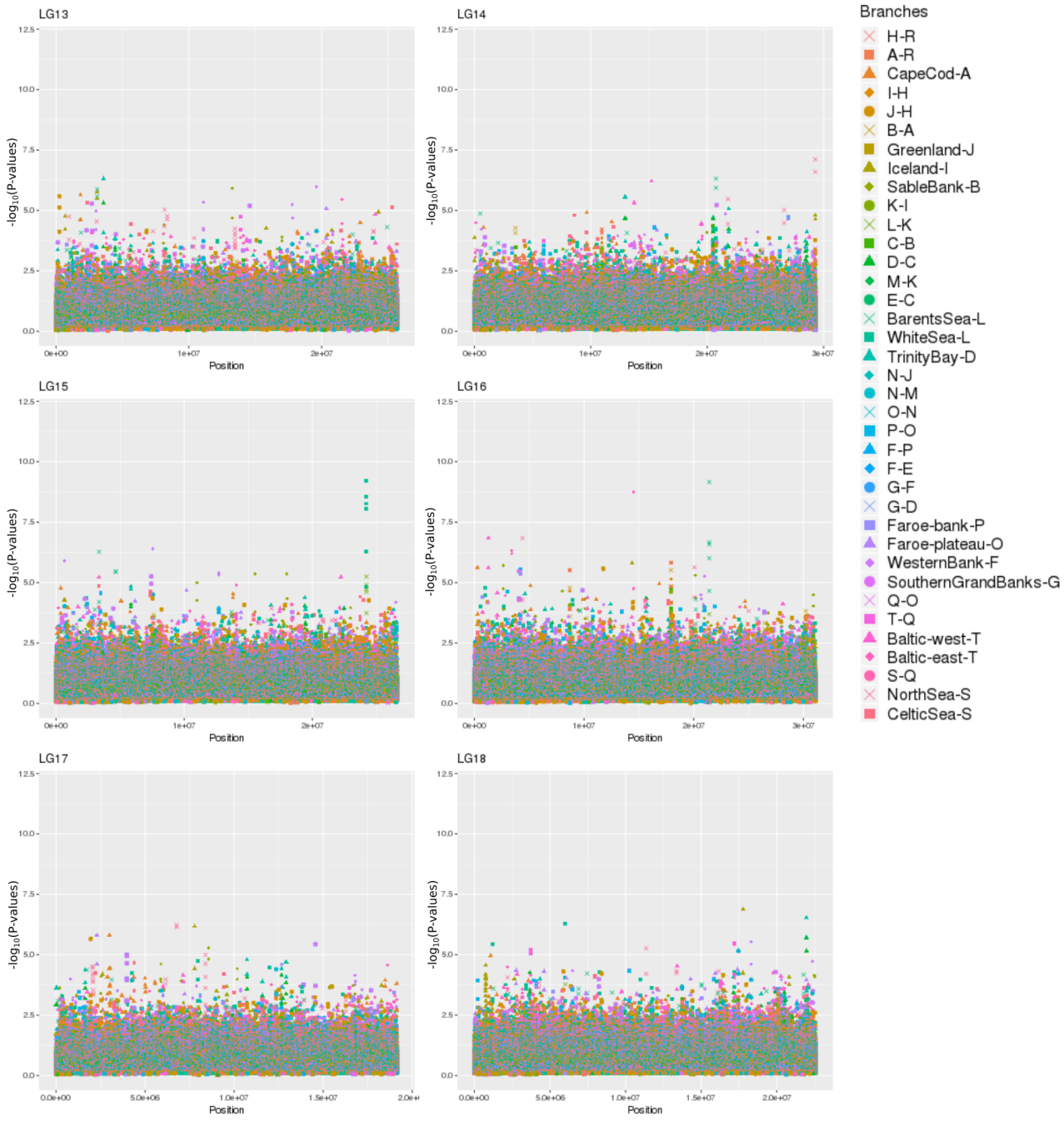

Figure S27: S_B scores for LG13 - LG18 in the Codfish data.

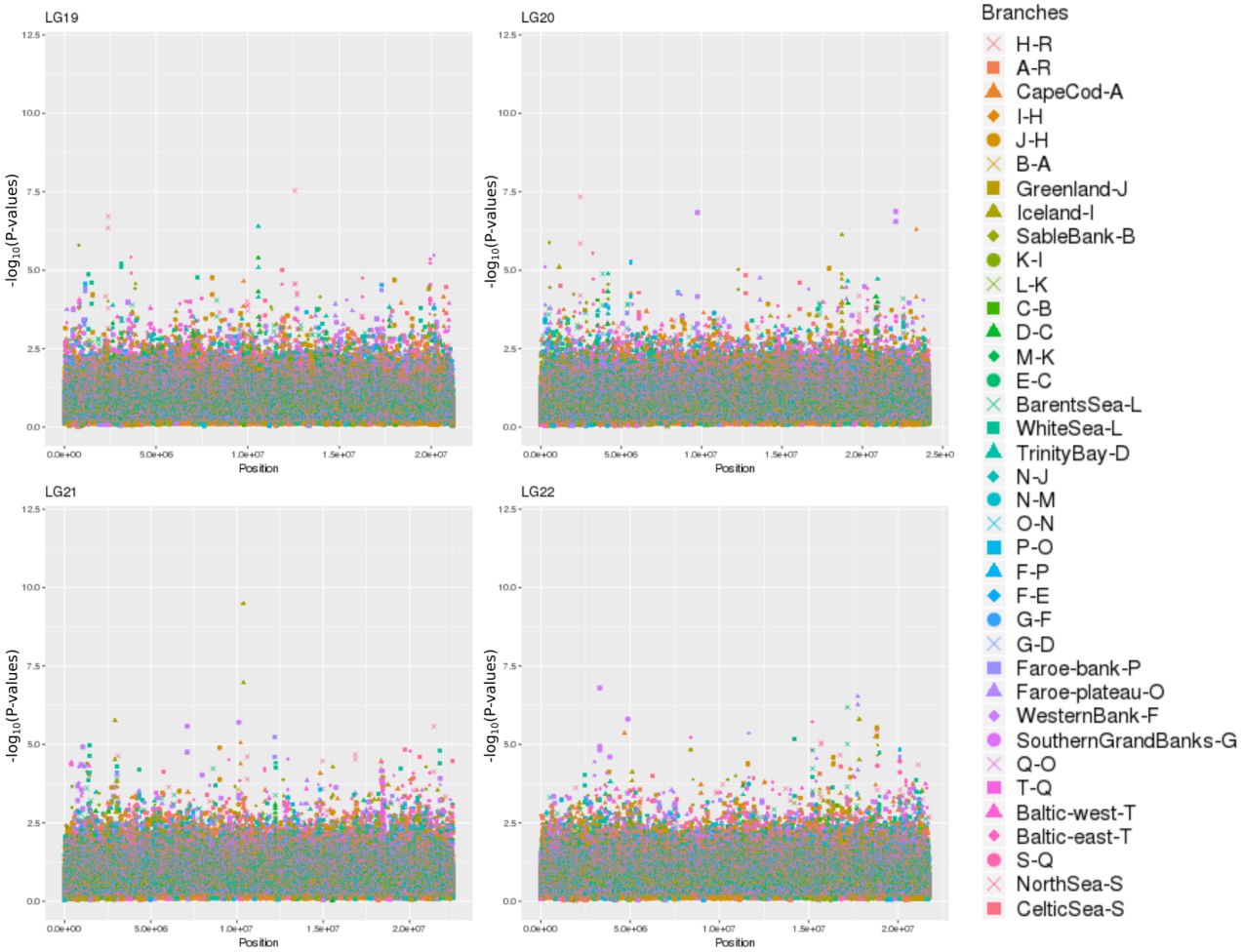

Figure S28: S_B scores for LG19 - LG22 in the Codfish data.

Supplemental Tables

Table S1: Proportion of observations under neutrality that are larger than the chi-squared statistic that would correspond to a particular P-value cutoff, computed for different branches of the graph from Figure S17.

P-value cutoff	0.05	0.01	0.001	1e-4	1e-5	1e-6
p2-R	0.068	0.023	0.0046	0.00067	3.2e-5	0
A-R	0.059	0.019	0.004	0.00032	0	0
C-A	0.046	0.011	0.001	0.00016	0	0
D-C	0.058	0.019	0.0034	6e-4	0	0
B-A	0.042	0.012	0.0016	9.5e-5	0	0
p3-C	0.066	0.024	0.0048	0.0011	0.00045	0
p4-D	0.069	0.023	0.0048	0.00099	6.4e-5	0
p1-B	0.067	0.022	0.0053	8e-4	6.4e-5	0
E-B	0.06	0.018	0.0034	0.0012	0.00013	0
p5-E	0.068	0.024	0.006	0.0016	0.00045	9.5e-5
F-D	0.067	0.021	0.0038	0.00045	3.2e-5	0
F-E	0.067	0.021	0.0038	0.00045	3.2e-5	0
p6-F	0.067	0.021	0.0038	0.00045	3.2e-5	0

Table S2: Top candidate regions from 1000 Genomes scan.

BRANCH(ES)	CHR	START	END	BEST POSITION(S)	MAXIMUM SCORE	GENES (+/- 100kb)
CDX-t	14	106143847	106389176	106243847	13.109	*KIAA0125*
CEU-v	2	135272951	137305495	136707982	13.033	*MGAT5,TMEM163,ACMSD,CCNT2, MAP3K19,RAB3GAP1,ZRANB3,R3HDM1, UBXN4,LCT,MCM6,DARS,CXCR4*
CDX-t	14	105864438	106093254	105967202	9.396	*BRF1,PACS2,TEX22,MTA1,CRIP2, CRIP1,C14orf80,TMEM121*
CEU-v	15	28256859	28595956	28365618; 28356859	9.111	*OCA2,HERC2,GOLGA8F*
v-q	5	33851116	34051693	33951693	9.067	*ADAMTS12,RXFP3,SLC45A2, AMACR,C1QTNF3*
CEU-v	5	33851116	34051693	33951693	8.676	*ADAMTS12,RXFP3,SLC45A2, AMACR,C1QTNF3*
v-q	15	48292165	48585926	48426484	8.673	*SLC24A5,MYEF2,CTXN2,SLC12A1,DUT*
TSI-v	5	33851116	34051693	33951693	8.644	*ADAMTS12,RXFP3,SLC45A2, AMACR,C1QTNF3*
TSI-v	15	48292165	48585926	48426484	8.356	*SLC24A5,MYEF2,CTXN2,SLC12A1,DUT*
CEU-v	15	48292165	48585926	48426484	8.214	*SLC24A5,MYEF2,CTXN2,SLC12A1,DUT*
v-q	17	4300392	4500392	4400392	7.912	*UBE2G1,SPNS3,SPNS2,MYBBP1A,GGT6, SMTNL2,ALOX15,PELP1*
CEU-v	4	38698648	38898648	38798648	7.815	*KLF3,TLR10,TLR1,TLR6,FAM114A1,TMEM156*
TSI-v	17	4300392	4500392	4400392	7.734	*UBE2G1,SPNS3,SPNS2,MYBBP1A,GGT6, SMTNL2,ALOX15,PELP1*
CEU-v	9	16692200	16902118	16800341	7.598	*BNC2*
CEU-v	17	4300392	4500392	4400392	7.389	*UBE2G1,SPNS3,SPNS2,MYBBP1A,GGT6, SMTNL2,ALOX15,PELP1*
TSI-v	17	18823818	19023818	18923818	7.382	*PRPSAP2,SLC5A10,FAM83G,GRAP,GRAPL,EPN2*
TSI-v	17	19074874	19399144	19239432	7.35	*GRAPL,EPN2,B9D1,MAPK7,MFAP4, RNF112,SLC47A1*
v-q	17	18823818	19023818	18923818	7.326	*PRPSAP2,SLC5A10,FAM83G,GRAP,GRAPL,EPN2*
v-q	17	19053175	19399144	19174874	7.323	*GRAPL,EPN2,B9D1,MAPK7,MFAP4, RNF112,SLC47A1*
TSI-v	20	31031309	31252094	31152094	7.113	*ASXL1,C20orf112,COMMD7,DNMT3B*
CDX-t	4	17713761	17913762	17813761; 17813762	7.027	*MED28,FAM184B,DCAF16,NCAPG,LCORL*

Table S3: Top candidate regions from Human Origins scan.

BRANCH(ES)	CHR	START	END	BEST POSITION(S)	MAXIMUM SCORE	GENES (+/- 100kb)
EastAsian-v	1	234527890	234735790	234635790	8.712	*SLC35F3,COA6,TARBP1,IRF2BP2*
EastAsian-v	11	119993920	120272688	120164246; 120164903; 120164954; 120165302	8.625	*TRIM29,OAF,POU2F3,TMEM136, ARHGEF12*
EastAsian-v	17	72925996	73163811	73063811	8.238	*SUMO2,NUP85,GGA3,TMEM104, GRIN2C,FDXR,MRPS7,FADS6, USH1G,OTOP2,MIF4GD,OTOP3,HID1, CDR2L,ICT1,KCTD2,ATP5H, SLC16A5,ARMC7,NT5C,HN1*
EastAsian-v	16	89576635	89847265	89694907; 89695266	7.905	*ANKRD11,SPG7,RPL13,CPNE7, DPEP1,CHMP1A,SPATA33,CDK10, SPATA2L,VPS9D1,ZNF276,FANCA, SPIRE2,TCF25*
w-y; w-x; European-w	4	38645482	38865720	38745482	7.869	*KLF3,TLR10,TLR1,TLR6,FAM114A1*
w-y; w-x; European-w	2	136879530	137129668	136981210; 136979530	7.868	*CXCR4*
w-y; w-x; European-w	5	33851693	34051693	33951693	7.8	*ADAMTS12,RXFP3,SLC45A2,AMACR, C1QTNF3*
NativeAmerican-x	3	119728374	120083940	119881691; 119887721	7.658	*GSK3B,GPR156,LRRC58,FSTL1*
NativeAmerican-x	16	11260583	11572138	11360583	7.658	*CLEC16A,RMI2,SOCS1,TNP2,PRM3, PRM2,PRM1,LITAF*
EastAsian-v	13	74026534	74264642	74136907; 74136940; 74137131	7.616	*KLF12*
EastAsian-v	22	42776791	42978831	42876791; 42878831	7.605	*TCF20,NFAM1,RRP7A,SERHL2, POLDIP3,CYB5R3,ATP5L2*
x-v	3	119728374	120083940	119881691; 119887721; 119983940	7.437	*GSK3B,GPR156,LRRC58,FSTL1*
x-v	16	11260583	11513302	11360583	7.437	*CLEC16A,RMI2,SOCS1,TNP2, PRM3,PRM2,PRM1*
NativeAmerican-x	12	30976944	31176944	31076944	7.358	*CAPRIN2,TSPAN11,DDX11*
w-y; w-x; European-w	15	48326484	48526484	48426484	7.332	*SLC24A5,MYEF2,CTXN2,SLC12A1,DUT*
y-q	15	48326484	48526484	48426484	7.323	*SLC24A5,MYEF2,CTXN2,SLC12A1,DUT*
NativeAmerican-x	14	21538319	21747765	21638319; 21647765	7.306	*METTL17,SLC39A2,NDRG2,TPPP2, RNASE13,RNASE7,RNASE8,ARHGEF40, ZNF219,TMEM253,OR5AU1,HNRNPC, RPGRIP1,SUPT16H*
NativeAmerican-x	14	47633244	47870258	47733244	7.263	*MDGA2*
x-v	14	47633244	47870258	47733244	7.257	*MDGA2*
EastAsian-v	2	48123015	48337869	48237869	7.251	*MSH6,FBXO11*
EastAsian-v	3	138824073	139070998	138969652; 138970998	7.232	*PRR23A,MRPS22,PRR23B,PRR23C,COPB2*
x-v	12	30976944	31176944	31076944	7.145	*CAPRIN2,TSPAN11,DDX11*
x-v	14	21538319	21747765	21638319; 21647765	7.122	*METTL17,SLC39A2,NDRG2,TPPP2, RNASE13,RNASE7,RNASE8,ARHGEF40, ZNF219,TMEM253,OR5AU1,HNRNPC, RPGRIP1,SUPT16H*
EastAsian-v	16	11265643	11466258	11365643	7.106	*CLEC16A,RMI2,SOCS1,TNP2,PRM3, PRM2,PRM1*
EastAsian-v	16	48275777	48482522	48375777; 48382522	7.045	*ABCC12,ABCC11,LONP2,SIAH1,N4BP1*
NativeAmerican-x	14	77516061	77719186	77619186	7.034	*IRF2BPL,CIPC,TMEM63C,ZDHHC22, NGB,POMT2,GSTZ1,TMED8*

Table S4: Country, sample sizes and data type for panels of cattle breeds analyzed in this study.

Abbreviation	Breed name	Country or region	Sample size	Data type	Reference
ALT	Alentejana	Portugal	6	shotgun	da Fonseca et al. 2019
ARO	Arouquesa	Portugal	6	shotgun	da Fonseca et al. 2019
BAR	Barrosã	Portugal	6	shotgun	da Fonseca et al. 2019
BC	Berrenda en colorado	Spain	3	777K chip	Upadhyay et al. 2017
BK	Boskarin	Hungary	4	777K chip	Shaheen et al. 2015
BN	Berrenda en negro	Spain	3	777K chip	Upadhyay et al. 2017
BRA	Brava de Lide	Portugal	6	shotgun	da Fonseca et al. 2019
BS	Brown Swiss	Switzerland	4	777K chip	Upadhyay et al. 2017
BU	Busha	Balkan region	6	777K chip	Upadhyay et al. 2017
CA	Cachena	Portugal	3	777K chip	Upadhyay et al. 2017
CCIBR	Cardena	Spain	5	777K chip	Upadhyay et al. 2017
CH	Chianina	Italy	3	777K chip	Upadhyay et al. 2017
DAM	N'Dama	Africa	10	shotgun	Kim et al. 2017
DB	Dutch Belted	The Netherlands	2	777K chip	Upadhyay et al. 2017
DF	Dutch Friesian	The Netherlands	4	777K chip	Upadhyay et al. 2017
EL	English Longhorn	England	4	777K chip	Upadhyay et al. 2017
FL	Fleckvieh	Switzerland	4	777K chip	Upadhyay et al. 2017
GA	Galloway	Scotland	5	777K chip	Upadhyay et al. 2017
GW	Groningen Whiteheaded	The Netherlands	5	777K chip	Upadhyay et al. 2017
HE	Heck	Germany	5	777K chip	Upadhyay et al. 2017
HOL	Holstein	The Netherlands	10	shotgun	Kim et al. 2017
JER	Jersey	Jersey Island	9	shotgun	Kim et al. 2017
KC	Kerry Cattle	Ireland	4	777K chip	Upadhyay et al. 2017
LI	Lidia	Spain	3	777K chip	Upadhyay et al. 2017
LM	Limia	Spain	4	777K chip	Upadhyay et al. 2017
MA	Maremmana	Italy	5	777K chip	Upadhyay et al. 2017
MER	Mertolenga	Portugal	6	shotgun	da Fonseca et al. 2019
MIR	Mirandesa	Portugal	6	shotgun	da Fonseca et al. 2019
MR	Meuse-Rhine-Yssel	The Netherlands	4	777K chip	Upadhyay et al. 2017
MRO	Maronesa	Portugal	6	shotgun	da Fonseca et al. 2019
MT	Maltese	Malta	4	777K chip	Upadhyay et al. 2017
PA	Pajuna	Spain	6	777K chip	Upadhyay et al. 2017
PRE	Preta	Portugal	6	shotgun	this study
RO	Romanian grey	Romania	4	777K chip	Upadhyay et al. 2017
SA	Sayaguesa	Spain	5	777K chip	Upadhyay et al. 2017
WP	White Park	England	3	777K chip	Upadhyay et al. 2017

Table S5: Top candidate regions from bovine selection scan, computing 1 score per SNP. Gene annotations were extracted from the Human Gene Nomenclature Committee (HGNC) and the Vertebrate Gene Nomenclature Committee (VGNC). We labeled windows with particularly low coverage in the target population, as the signal of selection may be inflated in those windows for that reason.

BRANCH(ES)	CHR	START	END	BEST POSITION(S)	MAXIMUM SCORE	GENES (HGNC)	GENES (VGNC)	NOTES
MA-B	7	31139786	31656058	31239786	15.955	N/A	*CSNK1G3,CEP120*	
BK-C	16	68131085	68331085	68231085	15.955	N/A	*HMCN1*	
HOL-P	10	38352236	38552236	38452236	15.955	N/A	*UBR1,TMEM62, CCNDBP1,EPB42*	
BU-E	4	90338939	90538939	90438939	15.955	N/A	N/A	
BRA-AA	14	43030034	43230034	43130034	15.654	N/A	N/A	
FL-I	6	89409731	89609731	89509731	13.564	N/A	*ADAMTS3*	
EL-O	21	13575619	13775619	13675619	13.322	N/A	N/A	low coverage
MIR-CC	1	22756273	22956273	22856273	12.643	N/A	N/A	
BU-E	6	39795259	39995259	39895259	12.327	N/A	N/A	
S-Q	16	32083264	32283264	32183264	12.095	*KIF26B*	*SMYD3*	
DF-RR	13	39876995	40076995	39976995	11.932	N/A	*RIN2,CRNKL1, CFAP61*	
LM-EEE	6	12117949	12317949	12217949	11.91	N/A	*UGT8*	
MT-CCC	2	10248519	10448519	10348519	11.852	N/A	N/A	
KC-M	1	29992983	30192983	30092983	11.766	N/A	N/A	
DF-RR	24	10629225	10829225	10729225	11.708	N/A	N/A	
MA-B	15	43161704	43361704	43261704	11.52	N/A	*SBF2*	
MER-EE	16	10597064	10797064	10697064	11.365	N/A	N/A	
EEE-CC	6	12117949	12317949	12217949	11.257	N/A	*UGT8*	
MER-EE	1	74866383	75066383	74966383	11.199	N/A	*ATP13A5,HRASLS*	
KC-M	2	110048350	110248350	110148350	11.103	N/A	N/A	
CCIBR-II	18	19615837	19815837	19715837	11.073	N/A	*SALL1*	
RO-F	17	38455167	38655167	38555167	10.932	N/A	N/A	
GW-S	16	20402906	20602906	20502906	10.924	N/A	*USH2A,ESRRG*	
BK-C	15	45459239	45659239	45559239	10.834	*OVCH2, PPFIBP2*	*CYB5R2*	
BS-I	12	46363654	46563654	46463654	10.811	N/A	N/A	
GW-S	16	32083264	32283264	32183264	10.804	*KIF26B*	*SMYD3*	
MA-B	8	53567800	53882133	53667800; 53782133	10.757	N/A	*GNA14,GNAQ*	
MT-CCC	8	71550088	71750088	71650088	10.736	*ENTPD4, SLC25A37*	*NKX3-1,NKX2-6*	
CH-A	26	35786475	35986475	35886475	10.725	*ATRNL1*	*TRUB1*	
EL-O	1	130658644	130858644	130758644	10.638	N/A	*KPNA6,RBP1,TXLNA, RBP2,COPB2,MRPS22*	
DAM-AAA	10	78830979	79030979	78930979	10.63	N/A	*GPHN*	
RO-F	8	86936023	87136023	87036023	10.613	N/A	*ZNF169,SPTLC1*	
MR-S	16	72485715	72685715	72585715	10.595	N/A	*RPS6KC1,ANGEL2, VASH2,SPATA45, TATDN3,NSL1,BATF3*	
MIR-CC	21	53764830	53964830	53864830	10.491	N/A	N/A	
CCC-D	2	10248519	10448519	10348519	10.452	N/A	N/A	
BK-C	15	43569293	43769293	43669293	10.385	N/A	*SBF2,WEE1,IPO7*	
MR-S	4	38360883	38560883	38460883	10.325	N/A	N/A	
MT-CCC	26	27532931	27732931	27632931	10.289	N/A	*SORCS1*	
GW-S	5	11395138	11595138	11495138	10.279	N/A	N/A	low coverage
BRA-AA	2	44270382	44470382	44370382	10.271	N/A	*ARL5A,NEB*	
BU-E	4	30182568	30382568	30282568	10.24	*DNAH11*	*SP4*	
AA-Z	14	43030034	43230034	43130034	10.194	N/A	N/A	
MT-CCC	7	25472570	25672570	25572570	10.131	N/A	*CHSY3,KIAA1024L, ADAMTS19*	
DAM-AAA	9	32434348	32634348	32534348	10.088	N/A	*FAM184A,MCM9, ASF1A*	
WP-O	14	48680437	48880437	48780437	10.079	N/A	*EXT1,MED30*	
CCIBR-II	5	6754684	6954684	6854684	10.001	N/A	N/A	

Table S6: Top candidate regions from bovine selection scan, computing score in windows of 10 SNPs with a step size of 1 SNP. Gene annotations were extracted from the Human Gene Nomenclature Committee (HGNC) and the Vertebrate Gene Nomenclature Committee (VGNC).

BRANCH(ES)	CHR	START	END	BEST POSITION(S)	MAXIMUM SCORE	GENES (HGNC)	GENES (VGNC)
RO-F	7	50851861	55066221	52810086	4.665	*FAM13B,BRD8,SMIM33, NRG2,PCDHA3,PCDHA6, PCDHA11,PCDHB1,PCDHB4, PCDHB6,PCDHB7,PCDHB16, PCDHB14,PCDHGA3,PCDHGB1, PCDHGB2,PCDHGA5,PCDHGA7, ARAP3*	*KLHL3,HNRNPA0,PKD2L2, WNT8A,NME5,KIF20A, CDC23,GFRA3,CDC25C, FAM53C,KDM3B,REEP2, EGR1,ETF1,HSPA9, CTNNA1,LRRTM2,SIL1, PAIP2,SLC23A1, MZB1,PROB1,DNAJC18, TMEM173,UBE2D2,CXXC5, PSD2,PURA, CYSTM1,PFDN1,HBEGF, SLC4A9,SRA1,APBB3, SLC35A4,CD14,TMCO6, IK,WDR55,DND1, HARS,HARS2,ZMAT2, TAF7,RELL2,PCDH1, DELE1,RNF14, GNPDA1,NDFIP1*
MA-B	7	30014797	32458116	31691420	4.511	N/A	*ZNF608,CSNK1G3,CEP120, PRDM6,PPIC,SNX24, SNX2*
MT-CCC	14	51034878	52622208	51623748	3.641	N/A	*TRPS1*
HE-G	3	94028894	97100382	95726532	3.461	N/A	*SCP2,ZYG11A,ZYG11B, COA7,SHISAL2A,GPX7, ZCCHC11,PRPF38A,ORC1, CC2D1B,ZFYVE9, ZFYVE9,BTF3L4,BTF3L4, TXNDC12,RAB3B,NRDC, OSBPL9,EPS15,TTC39A, RNF11,CDKN2C,FAF1, DMRTA2,ELAVL4*
DAM-AAA	8	57274558	59955508	57999794	3.379	*TLE1*	*PHF24,VCP,FANCG, PIGO,STOML2,FAM214B*
BU-E	4	89770514	91520720	90278376	3.263	N/A	*GPR37,POT1*
CCC-D	14	51034878	52277825	51623748	3.231	N/A	*TRPS1*
MT-CCC	2	10211900	11248899	10730400	3.185	*FSIP2*	N/A
LM-EEE	6	11322043	12843517	11882822	3.156	N/A	*NDST4,UGT8,ARSJ*
HOL-P	10	35129080	39547706	37761286	3.131	*CCDC9B,C15orf62,PLA2G4E*	*THBS1,FSIP1,GPR176, EIF2AK4,SRP14,BMF, BUB1B,ANKRD63,PLCB2, DISP2,KNSTRN, IVD,BAHD1,CHST14, CCDC32,RPUSD2,RAD51, RMDN3,GCHFR,DNAJC17, ZFYVE19,SPINT1,VPS18, DLL4,CHAC1,INO80, EXD1,CHP1,OIP5, NUSAP1,NDUFAF1,RTF1, ITPKA,RPAP1,TYRO3, MGA,MAPKBP1,SPTBN5, SPTBN5,EHD4,PLA2G4D, PLA2G4F,VPS39,TMEM87A, GANC,CAPN3, ZNF106,SNAP23,HAUS2, CDAN1,TTBK2, UBR1,TMEM62,CCNDBP1, EPB42*
FL-I	11	56815844	57798139	57361016	3.127	N/A	N/A
EEE-CC	6	11322043	12589046	11819996	3.004	N/A	*NDST4,UGT8*

Table S7: Area of sampling and sample sizes of Atlantic cod population panels analyzed in this study (see Figure S23).

Area	Population	Abbreviation	Sample size
US	Cape Cod	Cco	6
Nova Scotia	Western Bank	Web	5
Nova Scotia	Sable Bank	Sab	5
Newfoundland	Trinity Bay	Tri	4
Newfoundland	Southern Grand Banks	Sgb	4
Greenland	Greenland	Gre	11
Iceland	Iceland	Ice	61
Norway	Barents Sea	Bar	8
Faroes	Faroe Plateau	FarP	8
Faroes	Faroe Bank	FarB	5
Celtic Sea	Celtic Sea	Cel	8
North Sea	North Sea	Nse	12
Baltic Sea	Baltic West	BalW	8
Baltic Sea	Baltic East	BalE	8
Russia	White Sea	Whi	8

Table S8: Long high-differentiation regions in the Codfish data. Branches with corresponding scores with $-log_{10}(P) > 5$ for at least 1 SNP inside the region were placed into the column 'SIGNAL STRONG IN...'.

LINKAGE GROUP	START	END	SIGNAL STRONG IN...	SIGNAL ALSO PRESENT IN..
LG01	9.1Mb	26.1Mb	Iceland-I; BarentsSea-L	Greenland-J; J-H; K-I; M-K; N-J; N-M; O-N; Q-O
LG02	18.5Mb	24Mb	M-K; N-J; N-M; O-N; FaroePlateau-O; Iceland-I	NorthSea-S; S-Q; Q-O; K-I; L-K; CelticSea-S; C-B; FaroeBank-P; I-H; P-O
LG07	13.7Mb	23Mb	M-K; N-J; N-M; O-N; Iceland-I; K-I	A-R; B-A; BalticWest-T; C-B; P-O; Q-O; S-Q; T-Q; CelticSea-S; FaroeBank-P; FaroePlateau-O; H-R; I-H
LG12	0.5Mb	13.4Mb	CelticSea-S; Q-O; S-Q	Iceland-I; M-K; N-J; N-M; NorthSea-S; O-N